ARTICLE

https://doi.org/10.1590/2317-4889202120210031

BJGEO Brazilian Journal of Geology

Mineral potential re-evaluation of the Seis Lagos Carbonatite Complex, Amazon, Brazil

João Pedro Proença Bento[1]*, Claudio Gerheim Porto[1], Lucy Takehara[2], Francisco José da Silva[3], Artur Cezar Bastos Neto[4], Matheus Lamas Machado[1], Ana Carolina Duarte[1]

Abstract

The Seis Lagos Carbonatite Complex hosts a lateritic deposit developed over a siderite carbonatite. In the 1980's, it was estimated to contain 2.89 Bt @ 2.81 wt% Nb_2O_5. Recent studies have produced new data allowing re-evaluation of the area's mineral potential. In this work, a geological model has been constructed and new estimates of grades and tonnages are presented. The volume of cavities that occur in the lateritic crust is still unknown, and it was then segmented in possible scenarios ranging from 0 to 63%, impacting estimates of tonnage. The estimations were divided into two domains that vary according to the available data. In Domain 1, it has been estimated between 10.5-28.3 Mt @ 2.97 wt% Nb_2O_5 and 0.71 wt% REE_2O_3, and in Domain 2, between 1.40-3.78 Bt @ 1.17 wt% Nb_2O_5 and 0.46 wt% REE_2O_3. High grades of Ti, Sn and W were also detected for the lateritic crust. It is estimated that sediments in the Esperança Basin contain 11.8 Mt @ 1.76 wt% REE_2O_3 and 2.36 wt% P_2O_5, whereas the siderite carbonatite shows high grades of Nb, REE, Sc and Zn, further increasing the area's mineral potential. Soil grids on neighboring hills do not show similarly high Nb grades, but do present high grades of REE and P.

KEYWORDS: laterite; carbonatite; niobium; rare earth elements; Amazon; Brazil.

INTRODUCTION

Carbonatites are igneous rocks generally emplaced in stable continental terrains that contain at least 50% carbonate minerals and 20% silica (SiO_2) (Le Maitre 2002). According to Berger *et al.* (2009), these rocks are considered important sources of Niobium (Nb), Rare Earth Elements (REE) and phosphates (P_2O_5).

Carbonatites located in tropical regions are subjected to intense weathering that often develops thick lateritic regoliths associated to ferruginous crusts (Nahon and Tardy 1992). These regoliths may constitute important hosts of mineral deposits since the lateritization process can lead to supergenic enrichment of metals of economic interest (Freyssinet *et al.* 2005). According to Mitchell (2015), Nb deposits occur in primary carbonatites or their secondary counterparts, mainly associated to lateritic regoliths.

REE deposits may also be associated to the weathering of carbonatites or granites (Verplanck 2017). REE concentration in lateritic crusts over carbonatites may be increased tenfold in comparison to their protoliths (Chakhmouradian and Wall 2012). In addition, REE may occur adsorbed in clays in the regolith, such as the case of the Southern Chinese deposits (Kynicky *et al.* 2012). According to the International Union of Pure and Applied Chemistry (IUPAC), the REE family is composed of 17 metals including Scandium (Sc), Yttrium (Y) and the lanthanides. However, in this work, Sc is treated separately as it may behave differently (Williams-Jones and Vasyukova 2018). Most Sc deposits are found associated to alkaline and carbonatitic rocks in China and Russia (Williams-Jones and Vasyukova 2018). However, according to those authors, future production of Sc outside these countries may derive from lateritic regoliths.

Important Ti, Nb, P_2O_5 and REE deposits are associated to regoliths over the carbonatite complexes of Araxá, Catalão and Tapira, in the Alto Paranaíba Igneous Province (APIP) (Cordeiro *et al.* 2011). In the Amazon region, there are also important regolith caps covering carbonatite complexes such as Maicuru (Costa *et al.* 1991) and the focus of this work, the Seis Lagos Carbonatite Complex (SLCC).

The SLCC is located in the town of São Gabriel da Cachoeira, NW of the Amazonas State, Brazil (Fig. 1A). The surficial expression of this complex is given by three semicircular features that stand out as hills in the region's generally flat landscape. These hills are named Morro dos Seis Lagos (MSL); Morro do Meio (MM) and Morro do Norte (MN) (Fig. 1A). MSL contains a Nb deposit hosted in a lateritic crust with a thickness of more than 250 m developed over a siderite carbonatite (Giovannini *et al.* 2017, 2020).

[1]Universidade Federal do Rio de Janeiro – Rio de Janeiro (RJ), Brazil. E-mails: joao.proencabento@gmail.com, porto@geologia.ufrj.br, duarteanacarolina2@gmail.com, mattlamachado@gmail.com

[2]Companhia de Pesquisa de Recursos Minerais, Superintendência de Porto Alegre – Porto Alegre (RS), Brazil. E-mail: lucy.chemale@cprm.gov.br

[3]Universidade Federal Rural do Rio de Janeiro – Seropédica (RJ), Brazil. E-mail: fjosilva@yahoo.com

[4]Universidade Federal do Rio Grande do Sul – Porto Alegre (RS), Brazil. E-mail: artur.bastos@ufrgs.br

*Corresponding author.

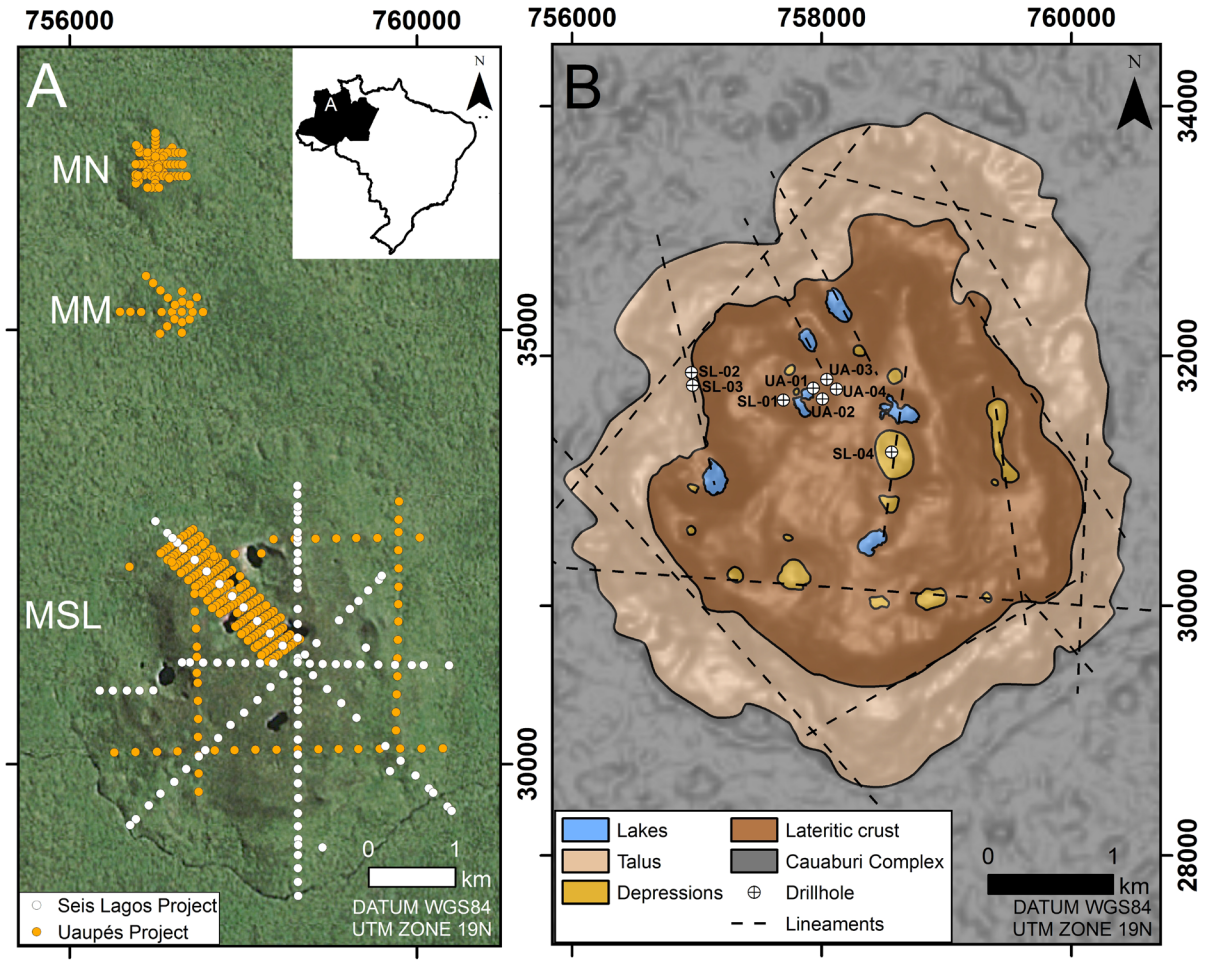

Figure 1. (A) Area location and satellite image showing "Morro do Norte" (MN); "Morro do Meio" (MM); "Morro dos Seis Lagos" (MSL) and the soil grids. (B) Geological map of MSL made in this work.

The Brazilian Geological Survey (CPRM) holds the the area's mineral rights and has conducted all exploration work since the discovery in the 70's. It has implemented the Seis Lagos Project (Viegas Filho and Bonow 1976) followed by the Uaupés Project (Justo 1983), that estimated total resources in the order of 2.89 Bt @ 2.81 wt% Nb_2O_5, ranking it as the world's largest Nb deposit (Chakhmouradian *et al.* 2015). However, after the discovery, the area has been declared a biological conservational unit as well as an indigenous reserve, preventing its economic exploitation. Despite these reasons, CPRM has retaken exploration in the area in 2012 as part of the Project "Evaluation of the REE potential in Brazil", which is referred to in this work as the "REE Project". In this Project, new analytical data have been generated utilizing archive samples and pulps (Takehara 2019) which allowed for a re-evaluation of the mineral resources in the area and the results are reported here.

This re-evaluation is justified since the resource estimation done by Justo (1983) was based on very low drill core recovery (29 to 61%). This is likely due to the large volume of cavities in the lateritic crust, reflecting the strong karstification processes that have affected the MSL. A far greater number of samples were also assayed in a modern laboratory by more advanced analytical methods whose quality has been properly assessed. This has allowed for the verification of anomalous results revealed by the grid sampling and core samples for a variety of metals of economic interest (e.g., Fe, Ti, Mn, REE, Sn, W, P and Zn) detected by Viegas Filho and Bonow (1976).

This work aims to perform a re-evaluation of the SLCC economic potential based on treatment and interpretation of recent analytical and historical data. In order to achieve that, new tonnage and metal grades were estimated based on the construction of a new geological map of MSL accompanied by a 3D geological model upon which different scenarios have been defined, showing possible variations in the proportion of the volume of cavities in the lateritic crust. This has prompted a new classification of the Nb estimates for the MSL deposit which follows the best practices guided by the international codes for reporting mineral resources (CBRR, 2016).

EXPLORATION HISTORY

The discovery of the semicircular structures that compose the SLCC is attributed to the Radar da Amazônia Project (RADAM) (Pinheiro *et al.* 1976). These structures are associated to radiometric anomalies along with Fe and Mn occurrences, which culminated in the selection of the area for further exploration work to be conducted by CPRM, initially through the Seis Lagos Project (Viegas Filho and Bonow 1976). In this project, an extensive grid soil and crust samples were collected, and four vertical drill holes were executed, being

named sequentially from SL-01 to SL-04 (Fig. 1B). The grid mapping identified a lateritic crust as the main lithology (Fig. 1B). In the surroundings, at lower elevations, is a talus deposit whose contacts are characterized by abrupt scarps (Viegas Filho and Bonow 1976). Geochemical anomalies were detected for several metals, specially Nb and REE, both in the soil grid and drill core samples.

The subsequent Uaupés Project (Justo 1983), aimed to quantify Nb resources in MSL, carried out four additional vertical drill holes named sequentially from UA-01 to UA-04 (Fig. 1B). Soil grids were implemented over MM and MN and densified over MSL (Fig. 1A). These four holes, spaced 125 x 150 m apart, were drilled down to a depth between 80 and 112 m. Sampling was conducted taking continuous 5 m long cores for Nb analysis. These holes were planned to end at similar elevations (Relative Sea Level (RSL) = 197 m) to enable constructing an ore block model measuring 150 m x 125 m x 5 m, with each drill hole at its center. This rectangular shape represents an area of influence considering half the distance to the neighboring hole.

With these parameters, Justo (1983) defined measured reserves of Nb in the mineralized lateritic crust down to a depth extending 47 m below the end of each hole. This extension downwards is equivalent to half the average of the hole length and this was justified assuming a much thicker mineralized lateritic crust. As each hole ended at RSL = 197 m and considering this extension, the measured reserves include all blocks from surface down to RSL = 150 m (Fig. 2). The terrain surface limits the top of each surficial block and their volumes were calculated using the topographic survey conducted as part of the project. The Nb grade of each model block was considered to be the same grade obtained in each 5 m long core intervals analyzed.

The indicated reserve defined by Justo (1983) considered a lateral extension of 200 m from each measured reserve block following the same depth. The grade of each block of the indicated category was considered equal to the block of measured reserve at the same RSL. The inferred reserve was defined as the entire volume of lateritic crust in MSL between RSL = 195 m and 305 m. However, the presence of lake sediments and water were not discriminated. Justo (1983) claimed that it is an arbitrary compensation for at least part of the rest of the lateritic crust that occurs below, until RSL = 10 m as indicated by drill hole SL-01. As a result, total reserves have been defined as 2.89 Bt with an average grade of 2.81 wt% Nb_2O_5 (Tab. 1). The three reserve categories defined by Justo (1983) are represented in Fig. 2.

The volume to tonnage conversion was calculated using density measurements of 17 different types of lateritic crust samples randomly selected. These measurements were calculated in the CPRM LAMIN laboratory using the water volume displacement method and the average value obtained was 3.84 g/cm^3.

In 2012, CPRM resumed exploration in the area as part of the REE Project with partial results published by Takehara

Table 1. Grade and tonnage estimates made by Justo (1983).

Reserve Classification	Tonnage	Nb_2O_5 grade (%)
Measured	38,376,000	2.85%
Indicated	200,640,000	2.40%
Inferred	2,658,892,800	2.84%
Total	**2,897,908,800**	**2.81%**

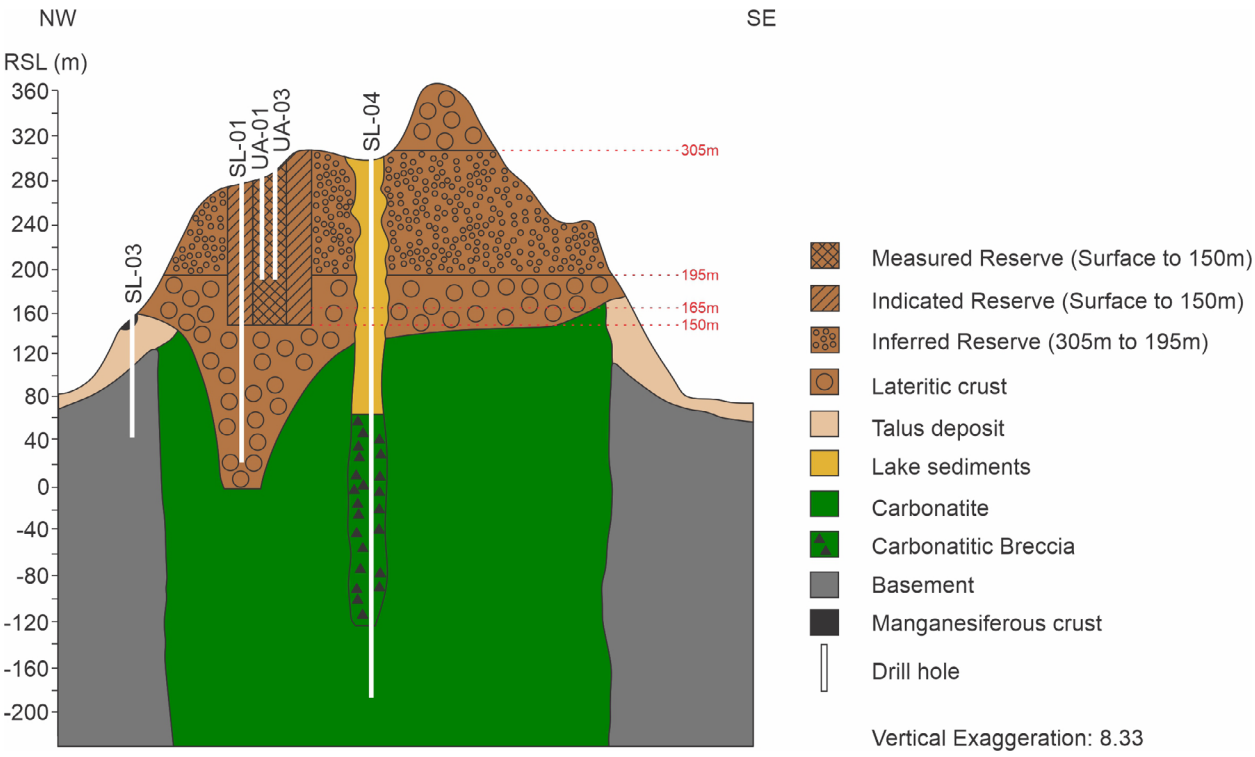

Source: modified from Justo (1983).

Figure 2. Schematic geologic profile of MSL showing the three reserve classifications defined by Justo (1983).

(2019). In this project, all drill hole cores (1,462.5 m) were re-logged and re-sampled, followed by new geochemical multielement analysis. In addition, all soil grid sample pulps were re-analyzed. This universe of new data composed the base upon which the mineral potential of MSL has been re-evaluated in the present work.

REGIONAL GEOLOGY

The SLCC lies in the Rio Negro Province's Imeri Domain in the Amazon Craton (CPRM 2006). The basement rocks of the Imeri Domain are represented by the Cauaburi Complex, dated at 1.8 Ga (Santos *et al.* 2000). Most common lithologies include migmatites, granites, gneisses, granodiorites and syenites that have been intensely weathered, resulting in regoliths at around 20 m thick (CPRM 2006). The positioning of the carbonatite intrusion was controlled by the intersection of a regional E-W structure longer than 400 km with two other minor NE-SW and NW-SE structures (Rossoni *et al.* 2016).

Rossoni *et al.* (2017) obtained three groups of U-Pb zircon ages from carbonatite samples: inherited zircons aged ~1820 Ma (compatible with the gneissic host rock crystallization); 1525 ± 21 Ma (upper intercept age); and 1328 ± 58 Ma (upper intercept age, MSWD = 1.4; Th/U from 1.52 to 0.14). The authors interpreted the 1328 ± 58 Ma age as the carbonatite's maximum age. The Rb-Sr and Sm-Nd isotopic data (Giovannini *et al.* 2020) suggest that the MSL's carbonatites can be much younger than the proposed age by Rossoni *et al.* (2017) and could be associated with the Penatecaua magmatism (200 Ma).

LOCAL GEOLOGY

The geological knowledge of MSL is based on the information obtained from eight diamond drill holes allied with geological mapping conducted during previous CPRM projects (Viegas Filho and Bonow 1976, Justo 1983) and more recent publications (Giovannini *et al.* 2017, 2020, Rossoni *et al.* 2016, 2017). Lateritic crusts intersected by drill hole SL-01 down to a depth of 255 m remain open since none of the other 4 drill holes have completely crossed it. Nevertheless, the cores of drill hole SL-01 could only be properly logged down to a depth of 100 m as the low recovery below only allowed discontinuous descriptions. Drill holes UA-01 to UA-04 intersected the mineralized lateritic crust down to a depth of 80 to 110 m, with similar characteristics of SL-01. These crusts present a porous and brechoidal structure cemented in iron oxy-hydroxides, representing a residual weathering product of the Fe rich siderite carbonatite. According to Lottermoser (1990), the formation of significant volumes of lateritic crust occur due to the intense circulation of superficial solutions as the carbonatite is oxidized and weathered, consequently losing volume. Giovannini *et al.* (2017) identified six different types of lateritic crust in drill hole SL-01 (Fig. 3): "Pisolitic Laterite"; "Fragmented Laterite"; "Mottled Laterite"; "Purple Laterite"; "Manganesiferous Laterite"; and "Brown Laterite". The first three types were collectively considered as reworked

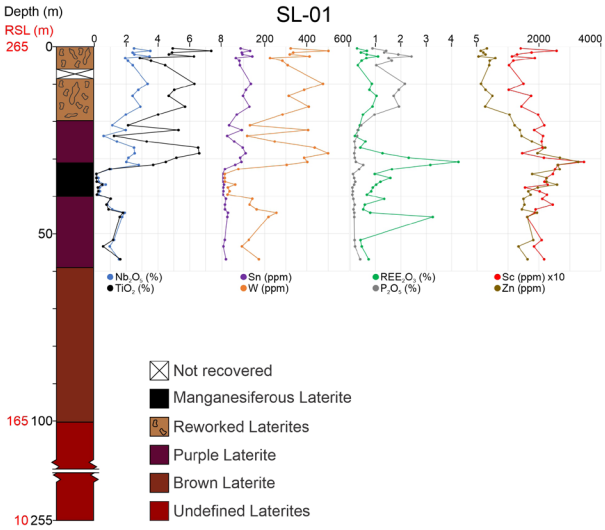

Figure 3. Geological profile of drill hole SL-01 and chemical elements distribution.

laterites, reflecting the effects of more recent alteration close to surface. Goethite and hematite constitute their main components. The "Manganesiferous Laterite" is composed of Mn oxides, mainly hollandite associated to cerianite. It occurs as discordant veinlets and irregular masses and has been interpreted as a late Mn precipitation event. Nb-rich rutile is the main Nb ore mineral identified across all types of lateritic crust. Giovannini *et al.* (2017) proposed that Nb-rich rutile was formed via the incorporation of Nb and Fe in the rutile structure replacing Ti. Other important minerals detected include Nb-brookite, florencite-(Ce) and more rarely, ankerite.

Drill holes SL-02 and SL-03 located close to the MSL's Northwestern border intersected the non-mineralized lateritic crust down to 15 m before reaching weathered granitic and gneissic, rocks, likely from the Cauaburi Complex. According to Giovannini *et al.* (2020), these lithologies are fenitized as they occur close to the carbonatite intrusion. Carbonatites were intersected by drill hole SL-02 at a depth between 221.60-227.70 m and are referred as "border siderite carbonatite" by Giovannini *et al.* (2020).

Drill hole SL-04 (Fig. 4) was placed at the center of the largest depression over MSL, named the Esperança Basin. From the surface down to 233.65 m it intersected various types of clay-rich lake sediments where palynological analysis indicated a Neogene age (2.58-23.03 Ma) (Viegas Filho and Bonow 1976). Kaolinite is the main constituent in all clay layers, with minor quartz, jarosite and florencite (Giovannini *et al.* 2017). Bonow and Issler (1980) identified anomalous REE grades associated to carbonaceous clay intervals between 14.65-73.00 m and estimated 7.8 Mt of ore with an average grade of 1.5 wt% REE_2O_3. Below the lake sediments, from 233.65 to 493.00 m, carbonatites were intersected and described by Giovannini *et al.* (2020) as "core siderite carbonatite" (233.65-288.00 m and 340.00-493.00 m) and "REE-rich core siderite carbonatite" (288.00-340.00 m). These rocks are variably friable, and their mineralogy is mainly constituted of siderite, barite and gorceixite, with minor rabdophane-(Ce) and pyrochlore. The "REE-rich core siderite carbonatite" contains

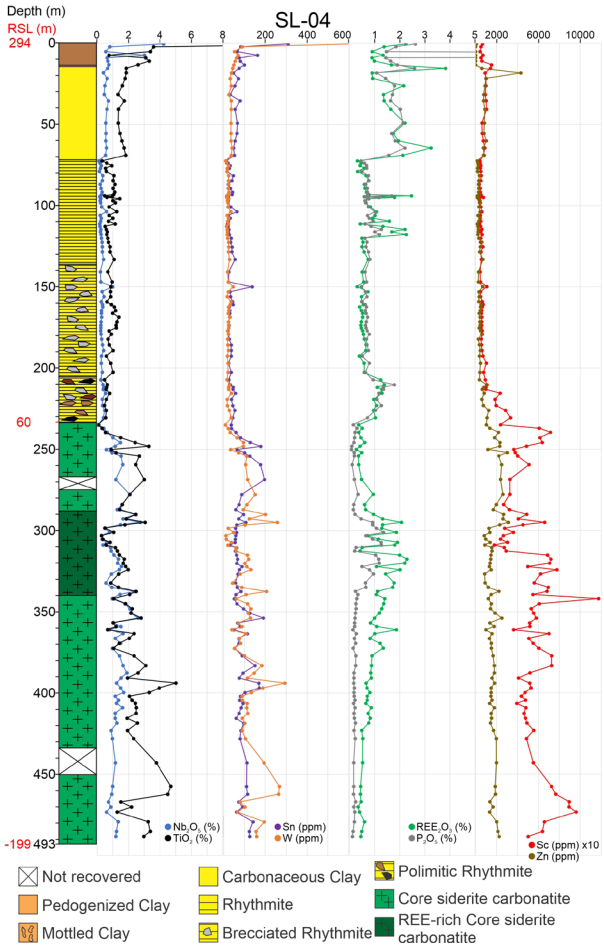

Figure 4. Geological profile of drill hole SL-04 and chemical elements distribution. The sediments described belong to Esperança Basin.

larger amounts of monazite and bastnäsite. The "core siderite carbonatite" is richer in Fe while the "border siderite carbonatite" is richer in Mn and P_2O_5.

METHODOLOGY

Sampling and geochemical analyses

All the sampling that took place in the SLCC was conducted by previous CPRM projects. This resulted in a database of 810 samples and pulps that were re-analyzed by the SGS Geosol Laboratory (Belo Horizonte, Brazil). Three analytical methods were applied:

- X-ray fluorescence (XRF) for 10 major oxides;
- ICP-MS combined with ICP-OES after metaborate fusion followed by acid dissolution and analysis for 14 REE plus Nb, Sn, W, Y and 11 other elements;
- ICP-MS combined with ICP-OES after aqua regia digestion and analysis for Sc, Zn and 23 other elements.

Analytical results below the lowest limit of detection were considered half of that value. Analytical results exceeding the upper limit of detection assumed that value, except in the cases of Nb, Pr, Sm, Nd, Ce and La, which were re-analyzed by XRF resulting in their respective oxides. It is important to mention that in the case of Nb, all drill holes and grid samples used to calculate tonnage and grade were analyzed via XRF. Nb results on soil grid in 18 samples above the upper detection limit of 4 wt% on XRF were corrected via a linear regression based on analytical results previously obtained on the same pulps by the Uaupés Project.

Certified reference materials and pulp replicates were inserted by the SGS lab in all analytical batches. These results were used in this work to evaluate analytical accuracy and precision for the analyses.

Geological map, model and elemental maps

A new geological map of MSL was produced based on the maps presented by Viegas Filho and Bonow (1976) and Rossoni *et al.* (2016). The first map was scanned and incorporated into GIS taking the six lakes as control points for georeferencing. The Rossoni *et al.* (2016) map was based on spectral band interpretation, resulting in a larger area of lateritic crust. These maps were then draped over the digital elevation model (DEM), produced using the Shuttle Radar Topographic Mission (SRTM) data with a resolution of 30 m/px, which is freely available on the Earth Explorer website, originally from the United States Geological Survey (USGS). Throughout this step, it was noticed that the past reported maps showed depressions and talus deposits over lateritic crusts. It is believed that the georeferencing procedure caused these inaccuracies since the lakes are concentrated in a small portion of the map, leaving the peripheral areas subjected to greater distortion. The eight drill holes and the soil grid also showed inaccurate coordinates that had to be adjusted following a similar procedure. A good positioning of the soil grid was obtained, as shown in Fig. 1A by its relative position to the lakes.

In order to produce the geological model, the logs of the eight drill holes were imported into Leapfrog Geo 4.5 along with the new geological map and the DEM. This model was enclosed by the following surfaces: at the top, by the topography (DEM); laterally, by the shape of MSL; at the base, by a plane cutting the Z axis at an arbitrary RSL of -200 m. All lithologies described by Justo (1983) and Giovannini *et al.* (2017, 2020) were grouped into the following units: basement; carbonatite; lateritic crust; manganesiferous crust; lake sediments; and talus deposit. As the drill hole logs did not define all the contacts between the lithologies (e.g., the contact between lateritic crust and carbonatite), the model was based not only on the drill hole logs, but also the geological map and the interpretation of the area presented by Justo (1983) (Fig. 2).

Hypothetical drill holes were created in order to assist the software in defining the contact surfaces between lithologies, for example: a sedimentary column analogous to the one found at SL-04 was created for all depressions and lakes; The contact between lateritic crust and carbonatite was assumed to occur 5 m below the base of SL-01, i.e., RSL = 5 m. According to Cowan *et al.* (2003), the explicit geological modeling consists of the use of maps and cross sections to produce the model according to the operator's geological interpretation of the area, while in the implicit geological modeling the software generates the contacts and bodies through the use of an algorithm. Therefore, these hypothetical drill holes are an adaptation

from an implicit-based software to an explicit-based model. This procedure has limitations but given the paucity of drill hole information of the area, we believe that it presents a valid way of conveying the conceptual geological model that the authors envisage for the MSL.

Elemental maps of the surface of the lateritic crust were produced using the geochemical results of the soil grid over MSL. Inverse Distance Weighting (IDW) was the data interpolation method applied, considering a search radius of 1200 m and 10-15 sample neighbors following the ArcGIS 10.4.1 default according to the data distribution of the grid. The interpolated data were classified based on natural breaks (Jenks) following the ArcGIS menu of options.

Grade and tonnage estimates

The volume of lateritic crust and lake sediments were estimated based on the geological model presented by the algorithms of the software. The lowest limit of the lateritic crust is unknown, however, to estimate its volume, its lowest limit considered was RSL = 165 m, which corresponds to drill hole SL-01's upper 100 m. Below 100 m, the core recoveries were extremely poor. The surface elevation was considered the upper limit of the model. The estimated volumes were then segmented in two. Domain 1 corresponds to the projection of the areas of influence (125 x 150 m) around each drill hole that intersected the lateritic crusts (UA-01 to UA-04 and SL-01), while Domain 2 corresponds to the remaining volume of lateritic crust in MSL above RSL = 165 m.

Since the drill core recoveries in the lateritic crusts was low (~37%) and it is unknown whether this is due to cavities formed by karstification, technical drilling issues or both, a plot was created to illustrate how the tonnages are estimated in a gradual scenario ranging from an ideal 0% to a maximum of 63% of cavities. In this case, the percentage of cavities are referred as the percentage of open spaces that cause poor core recovery and not the natural pores in the lateritic crust. An average density of 3.84 g/cm^3 was considered, as obtained by Justo (1983).

The total volume of lake sediments was estimated by the geological model, but special attention was given to the Esperança Basin. We considered an average density of 1.8 g/cm^3 for these sediments as reported by Bonow and Issler (1980). Although water masses were not modelled, an average depth of 4 m (Cordeiro *et al.* 2014) was considered in order to manually calculate its volume and then remove it from the total volume estimated by the geological model.

RESULTS

Analytical quality control

The analytical accuracy for Nb measured in the REE project was normalized to the GRE-03 standard (http://www.geostats.com.au), a barite carbonatite, with a certified value (CV) of 3524 ppm Nb (or 0.504 wt% Nb_2O_5). The control limits (CL) are set based on the dataset's standard deviation, and in this work, the concept of Thompson (1988) was followed where the standard deviation is defined as Eq. 1:

$$s_{e,ij} = (SDL_{ij} + \frac{\mu_{ij} \times RL_{ij}}{100\%})/3 \quad (1)$$

where:
$s_{e,ij}$: Standard Deviation for element *I* in analytical method *j*;
SDL: Statistical Detection Limit for element *i* in analytical method *j*;
RL: Repeatability Limit for the element *i* in analytical method *j*;
μ_{ij}: Concentration of the element *i* in analytical method *j*.

Both SDL and RL for Nb by XRF analyses were provided by the SGS Geosol lab (0.125% and 5 wt% Nb_2O_5, respectively). Considering μ_{ij} = 0.504 wt% Nb_2O_5, the standard deviation obtained is 0.05007. It was used to calculate the CL as plotted in Fig. 5 along with the results of 17 analysis of the GRE-03 standard by SGS. The average value of 0.502 wt% Nb_2O_5 sets a negligible analytical bias of -0.4%. All results are within the 95% confidence interval which points to the lack of bias in the analytical procedure.

The analytical variance of the REE Project was estimated from 16 analytical replicate pairs covering a grade range between 0.1 and 2.7 wt% Nb as plotted in Fig. 6 along with the "Reduced Major Axis" (RMA) line that is best adjusted to both data series (Sinclair and Bentzen 1998).

According to Sinclair and Bentzen (1998), the error (e) obtained by the RMA line (e = 0.025) can be expressed in terms of the variances of the two data series. Since these analyses were performed in the same laboratory under the same conditions, their variances are assumed to be equal, therefore (Eq. 2):

$$\begin{aligned} e^2_{REE\ PROJECT} &= s^2_{REP} + s^2_{SMP} \\ e^2_{REE\ PROJECT} &= 2(s^2_{REE\ PROJECT}) \\ s^2_{REE\ PROJECT} &= 0.000305 \\ s_{REE\ PROJECT} &= 0.017468 \end{aligned} \quad (2)$$

The analytical precision (P), according to Thompson and Howarth (1978), is related to the standard deviation (s) of a series of analytical replicated data and their concentration as follows (Eq. 3):

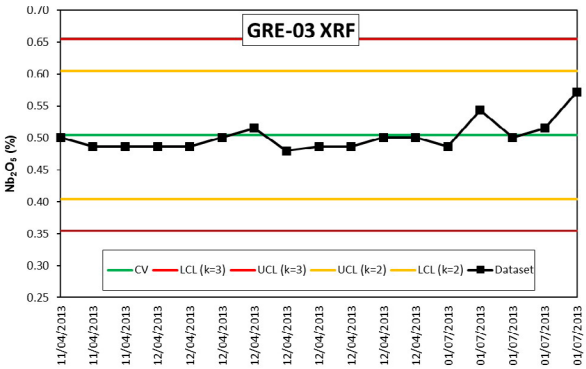

Figure 5. Black line: Nb_2O_5 results obtained by SGS Geosol. Green: GRE-03 standard certified value for Nb_2O_5 (0.504 wt%). Yellow lines define the 95% confidence interval = CV+/- 2s. Red lines define the 99.73% confidence interval = CV+/- 3s.

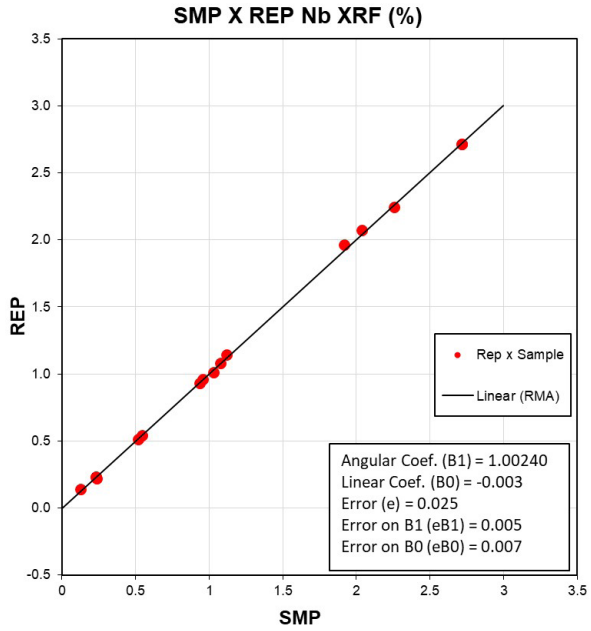

Figure 6. RMA line comparing XRF Nb (wt%) content in analytical replicate sample pairs of the SGS Geosol lab for the REE Project.

$$P\ (\%) = 200 * s / c \quad (3)$$

where:
P (%): analytical precision in %;
s: standard deviation;
c: concentration (average of all replicate pairs).

Concerning the replicate pairs average concentration of 1.16782 wt% Nb and the respective standard deviation of 0.017468, the analytical precision obtained by SGS-Geosol lab for Nb analysis by XRF for the REE Project is 2.99%, an excellent result.

The same procedure was applied to the replicate pairs of other metals that are considered the most relevant in the SLCC. The results listed in Tab. 2 show that precisions range from 2.99 to 8.44% except for Tm, Yb and Lu (that occur in very low concentrations) and for W, possibly due to the nugget effect.

The XRF Nb analyses conducted by the LAMIN/CPRM laboratory for the Uaupés Project (Justo 1983) do not report results for standards and replicates analyses, therefore accuracy and precision could not be determined. However, 70 core sample pulps of drill holes UA-01 to UA-04 were analyzed by LAMIN/CPRM laboratory were re-analyzed by SGS-Geosol laboratory for the REE Project. The results are plotted in Fig. 7 along with the RMA line, whose equation parameters can be seen along with their calculated errors. The equation that describes the RMA performed is Y = 1.0805x - 0.061, while the built-in error for the angular coefficient is 0.030. This shows that these data series represent statistically different populations since the value of the angular coefficient plus or minus its error does not include 1, in which case the line would fall in the range of the isovalue line (X = Y), also shown in the graph. It is possible to observe that the Nb results of the REE Project show an 8.05% grade increase in comparison to the Uaupés project. This represents a negative bias in the LAMIN lab since the SGS Lab results show no bias in comparison to the GRE-03 standard.

Table 2. Precision (%) of the most relevant metals in SLCC.

Metal	Method	Mean concentration	Precision (%)
Nb	XRF	1.17%	2.99
TiO_2	XRF	2.52%	3.31
P_2O_5	XRF	0.99%	4.81
MnO	XRF	1.85%	4.00
Zn	Aq regia ICP	671 ppm	7.28
Sc	Aq regia ICP	258 ppm	7.22
Y	Fusion ICP	232 ppm	5.58
La	Fusion ICP	1484 ppm	5.75
Ce	Fusion ICP	2591 ppm	8.44
Pr	Fusion ICP	280 ppm	7.87
Nd	Fusion ICP	1234 ppm	5.83
Sm	Fusion ICP	293 ppm	6.23
Eu	Fusion ICP	78 ppm	6.24
Gd	Fusion ICP	144 ppm	6.42
Tb	Fusion ICP	14 ppm	7.30
Dy	Fusion ICP	165 ppm	6.63
Ho	Fusion ICP	21 ppm	5.36
Er	Fusion ICP	40 ppm	7.84
Tm	Fusion ICP	5 ppm	12.66
Yb	Fusion ICP	27 ppm	10.97
Lu	Fusion ICP	4 ppm	14.82
Sn	Fusion ICP	75 ppm	7.92
W	Fusion ICP	250 ppm	19.64

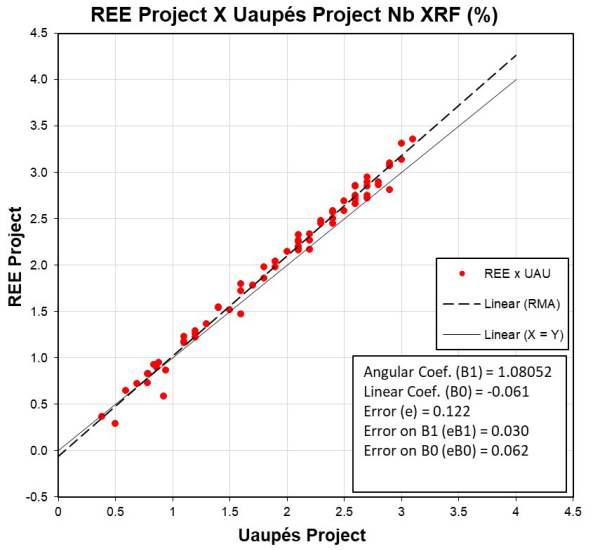

Figure 7. Nb contents from Uaupés and REE projects in the same pulps.

Geological map and 3D model

The new geological map is presented in Fig. 1B. The surface is dominated by lateritic crusts that occupy 8.13 km^2,

representing 48% more ground in comparison to the map elaborated by Viegas Filho and Bonow (1976). This is mainly due to the incorporation of the areas surrounding the lakes in the W and NW parts of the MSL (Fig. 8A). These areas correspond to carbonatites that were either dissolved, forming karsts and lakes, or were subsequently lateritized, contributing to the area now covered by lateritic crusts.

The areas occupied by depressions have diminished in about 39% and represent 0.31 km². The Esperança Basin's area, the biggest and most important of them, is estimated at about 92,787 m², very close to the 89,727 m² estimated by Bonow and Issler (1980). In comparison to Rossoni *et al.* (2016)'s map, regardless of minor topographic adjustments and addition of depressions, the most important modification was the incorporation of isolated bodies of lateritic crusts located in the E and N portions of the MSL to the main body of lateritic crust (Fig. 8B). This is justified by the lack of any abrupt topographic breaks that would otherwise suggest the existence of separated bodies of lateritic crusts.

Figure 9 shows the resulting 3D geological model and sections of MSL. In the absence of information that guides the lateral contacts between lateritic crust and lake sediments, we opted for modeling them as cylindrical bodies, which is possibly the closest model to represent channels whose dimensions and shapes are unknown in depth. The talus deposit was modelled as a blanket, following the topography at approximately 15 m thick. The manganesiferous crust was intersected by only 2 drill holes (UA-03 and SL-01) and could not be linked. In addition, these intersections do not share a similar thickness or even occur at the same RSL. Therefore, we opted to represent the manganesiferous crust as two separate oblate discs with constant thickness.

Metal grades in the soil grid

The geochemical grades of relevant metals from the soil grids over MSL, MM and MN are plotted in the boxplots of Fig. 10 for comparison. The Fe_2O_3 grades tend to be higher in MSL. Niobium is distinctly richer in MSL in comparison with MN and MM. On the other hand, REE grades are higher in MM and MN.

The correlations among some relevant metals in the lateritic crust over the MSL was studied using a Pearson correlation matrix (Tab. 3) and this was followed by the construction of contour maps (Fig. 11).

Fe_2O_3 shows a negative correlation with most other metals due to a closure effect. A strong correlation occurs among Nb, TiO_2, W and Sn (> 0.75) reflecting the close association of these metals in the structure of the Nb-rich rutile (Giovannini *et al.* 2017). The Nb map shows that in the central-NW portion of the MSL there is a high-grade zone coinciding with the area where drilling was concentrated. The presence of a neighboring Nb anomalous zone immediately to the east is also clear, where no drilling has been done to date.

P_2O_5, REE_2O_3 and Al_2O_3 also show good correlations (> 0.74). These components tend to concentrate in the vicinities of the Esperança Basin as shown in the P_2O_5 and REE_2O_3 maps in Fig. 11. This suggests that REE are associated to Al-phosphates in the surface lateritic crusts close to the Esperança Basin. Zinc do not show significant correlation with any other metal.

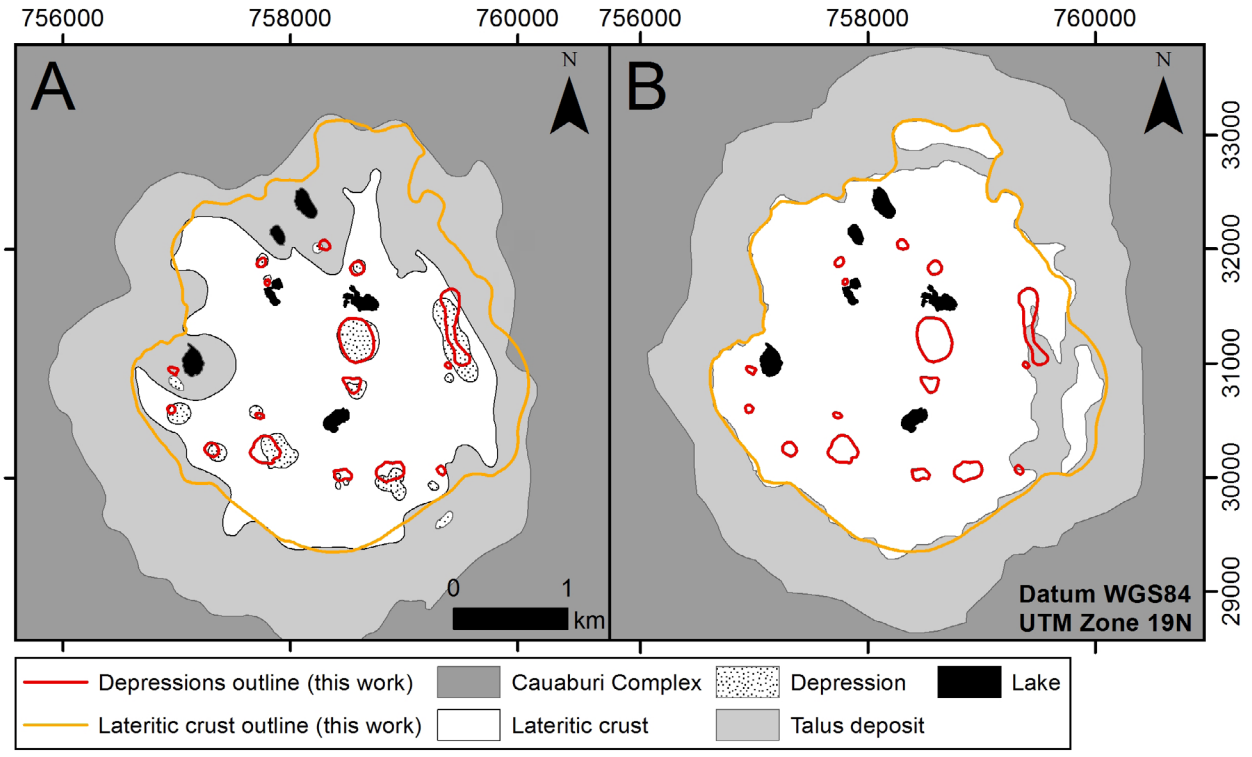

Figure 8. Comparison of the geological maps published for the Morro dos Seis Lagos area. (A) Viegas Filho and Bonow (1976). (B) Rossoni *et al.* (2016). Orange and Red lines are the contours of lateritic crust and depressions defined by the map produced by this work.

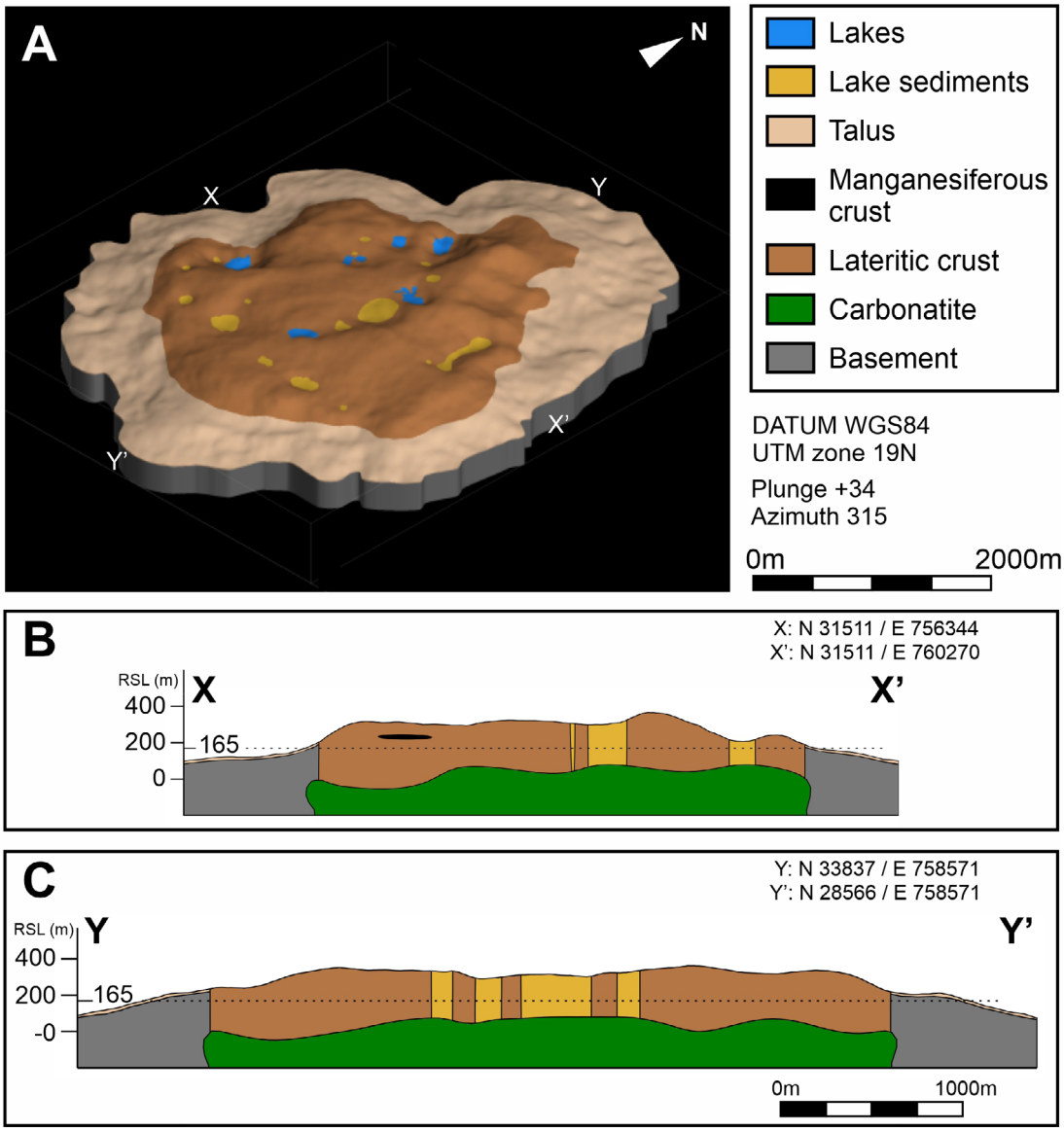

Figure 9. (A) Perspective view of MSL's geological model. (B) X-X' cross-section. (C) Y-Y' cross-section.

Metal grades at depth

Boxplots were produced in order to compare the distribution of metal grades between the following group of samples in MSL (Fig. 12): lateritic crusts of the soil grid; lateritic crust of the soil grid under the area of influence of drill holes; lateritic crusts of drill holes UA-01 to UA-04; manganesiferous crust; and siderite carbonatites. All siderite carbonatites come from drill hole SL-04.

Zinc in the lateritic crust is highly depleted when compared to the carbonatites. This leaching increases closer to surface (Fig. 3), however, it is highly enriched in the manganesiferous crust (median = 2,004 ppm Zn) reflecting the affinity of Zn with Mn oxides. The richest Zn interval occurs in the carbonatites from drill hole SL-04 between 238-297 m (Fig. 4), with a composite grade of 2,356 ppm. Further investigation is necessary in order to determine if Zn is hosted in sulfides or carbonates.

The REE grades in the lateritic crusts tend to be slightly lower compared to carbonatites where the SL-04 drillhole's 288 to 340 m interval ("REE-rich core siderite carbonatite") has a composite grade of 1.45 wt% REE_2O_3 (Fig. 4).

The P_2O_5 grades of the lateritic crusts (median = 0.91 wt%) and lake sediments (median = 0.75 wt%) are higher than the carbonatites. The REE_2O_3 / P_2O_5 ratio is higher in the carbonatites compared to the lake sediments, implying a distinct type of REE mineralization. Giovannini *et al.* (2020) reports the presence of florencite-(Ce) in the lake sediments and monazite and bastnäsite in the "REE-rich core siderite carbonatite".

Niobium median grades in the carbonatites (8,300 ppm) are similar to the lateritic crusts of the soil grid (8,150 ppm) but rise sharply to 22,000 ppm in the lateritic crusts from drill holes, going even further to 23,050 ppm in the lateritic crusts from the drill holes' area of influence. In addition, it can be noted that in all 5 holes drilled in the lateritic crusts, the Nb grades of the samples corresponding to reworked laterites are constantly higher if compared to the samples in the lower portions of the laterite profile as seen in the SL-01 log (Fig. 3). A similar pattern is observed for TiO_2, Sn and W.

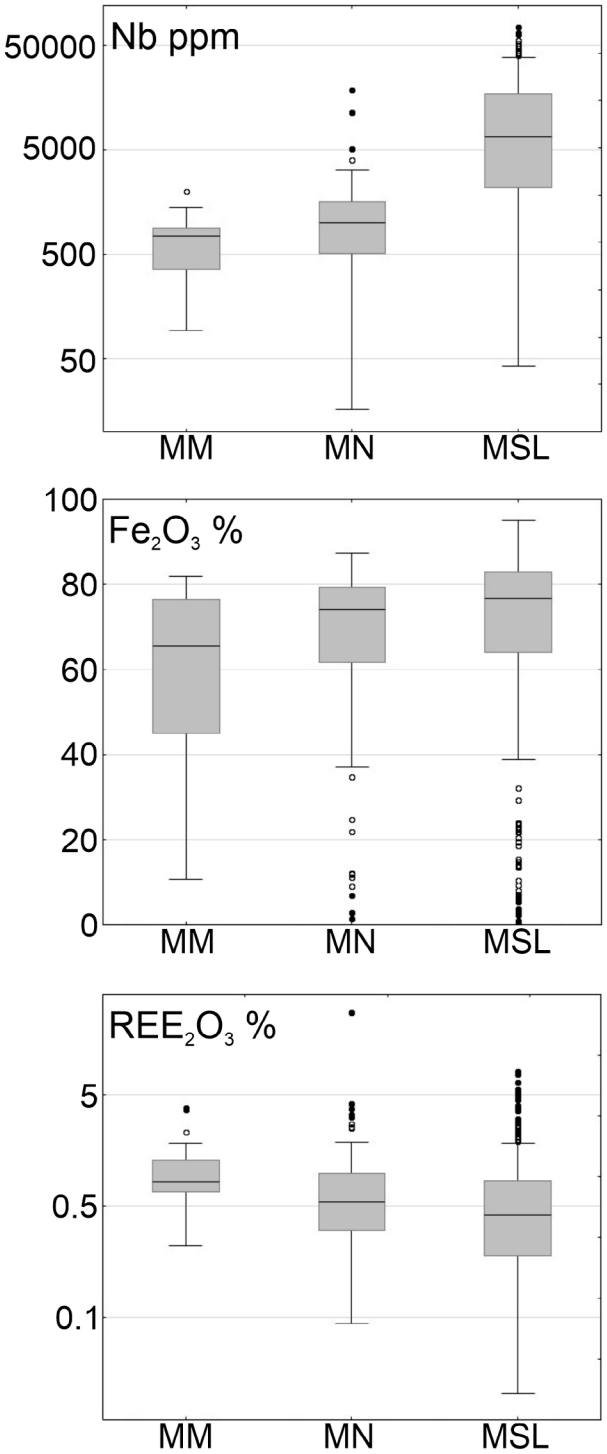

MM: Morro do Meio; MN: Morro do Norte; MSL: Morro dos Seis Lagos.

Figure 10. Boxplots comparing the grades of Fe2O3, Nb and REE2O3 between the three main structures that compose the SLCC. Open and closed circles represent outlier and extreme outlier values, respectively.

Grade and tonnage estimation in the lateritic crusts

In order to estimate the volume of mineralized lateritic crust at MSL, the geological model was cut at RSL = 165 m (Figs. 9B and 9C). This volume was measured within the Leapfrog software, resulting in 990,940,000 m^3 (equivalent to a total of 3.80 Bt assuming a density of 3.84 g/cm^3). Domain 1 contains a maximum of 28.3 Mt and encompasses the amount of lateritic crust within five drill holes' area of influence (Fig. 13A). For drill holes UA-01 to UA-04, the tonnage of lateritic crust is limited by the topographic surface down to the maximum depth reached by these drill holes (RSL = 197 m). For drill hole SL-01,the depth at which continuous sampling was possible was considered to be 58.75 m (RSL = 206 m). Domain 2 contains a maximum of 3.78 Bt and is characterized by the absence of drill holes in lateritic crusts (Fig. 13B). It contains all remaining lateritic crust in the MSL from surface down to RSL = 165 m.

The volume of lake sediments and manganesiferous crusts were modeled and measured separately from the above-mentioned Domains 1 and 2.

The five drill holes that intersected the lateritic crust showed an average recovery of 37% between surface and RSL = 165 m, but the volume of cavities is unknown. Given this lack of information, the model considered different scenarios where in one extreme all unrecovered material is assumed to be due to cavities, i.e., the total volume of cavities corresponding to 63% and on the other extreme, the low recovery is entirely due to the poor drilling performance. The graph presented in Fig. 14 depicts 7 different scenarios where the percentage of cavities ranges from 0% to a maximum of 63%. In this graph, the tonnage of lateritic crust in Domain 1 may vary from 10.5 Mt to 28.3 Mt and in Domain 2 from 1.40 Bt to 3.78 Bt.

The grades in Domain 1 were taken as the composite grade of the lateritic crust in each of the 5 drill holes (Tab. 4). For Domain 2, the average metal grades were estimated based on the median grades of the soil grid over the lateritic crusts (Tab. 4). The median grades of the soil grid in the drill holes' area of influence are also shown in Tab. 4 for comparison. It can be noted that the highest Nb grades occur in the soil grid restricted to the area of influence of the drill holes (3.30 wt% Nb_2O_5), followed by the drill holes (2.97 wt% Nb_2O_5) and by the entire soil grid (1.17 wt% Nb_2O_5). Ti, Sn and W follow a similar pattern. An opposite tendency is observed for the REE and P grades that are lower in the soil grid on the area of influence of the drill holes compared to the drill hole grades. This behavior, opposite to Nb, reflects the leaching tendency of REE and P near surface.

Grade and tonnage estimation of lake sediments

The modeled volume of the lake sediments was also segmented according to available data. In order to produce the geological model, it was considered that all lakes and depressions are filled by sediments similar to those found in the Esperança Basin, where SL-04 was drilled. The volume occupied by the Esperança Basin (21,475,000 m^3) corresponds to 23% of the total lake sediments modeled (91,453,708 m^3). The volume of mineralized clay sediments intersected from the surface to 71.90 m with a composite grade of 1.76 wt% REE_2O_3 and 2.36 wt% P_2O_5 is equivalent to 6,569,300 m^3, making up 7% of the total modeled volume of lake sediments. If a density of 1.8 g/cm^3 is considered, the tonnage of mineralized lake sediments at the Esperança Basin is estimated at 11.8 Mt.

Table 3. Pearson correlation matrix for soil grid samples over the lateritic crusts of MSL.

	Fe_2O_3	Al_2O_3	P_2O_5	Nb	TiO_2	Sn	W	REE_2O_3	Zn
Fe_2O_3	1.00	-	-	-	-	-	-	-	-
Al_2O_3	-0.48	1.00	-	-	-	-	-	-	-
P_2O_5	-0.46	**0.75**	1.00	-	-	-	-	-	-
Nb	-0.54	0.12	0.23	1.00	-	-	-	-	-
TiO_2	-0.58	0.13	0.22	**0.89**	1.00	-	-	-	-
Sn	-0.51	0.19	0.28	**0.75**	**0.79**	1.00	-	-	-
W	-0.53	0.09	0.19	**0.89**	**0.91**	0.66	1.00	-	-
REE_2O_3	-0.35	0.52	**0.74**	0.00	0.00	0.00	0.03	1.00	-
Zn	0.15	-0.35	-0.42	-0.18	-0.28	-0.32	-0.18	-0.19	1.00

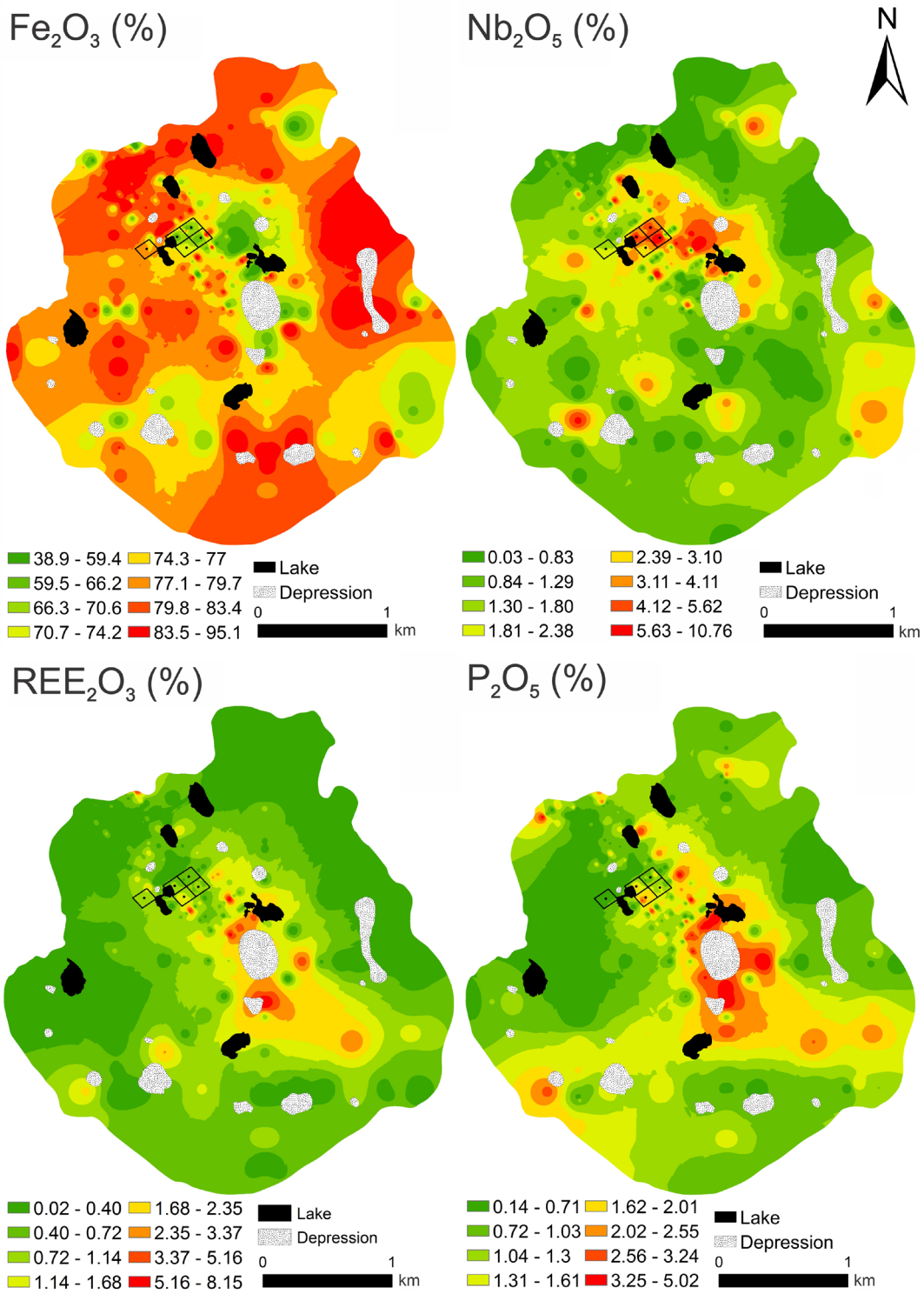

Figure 11. Isograde maps on MSL's lateritic crust.

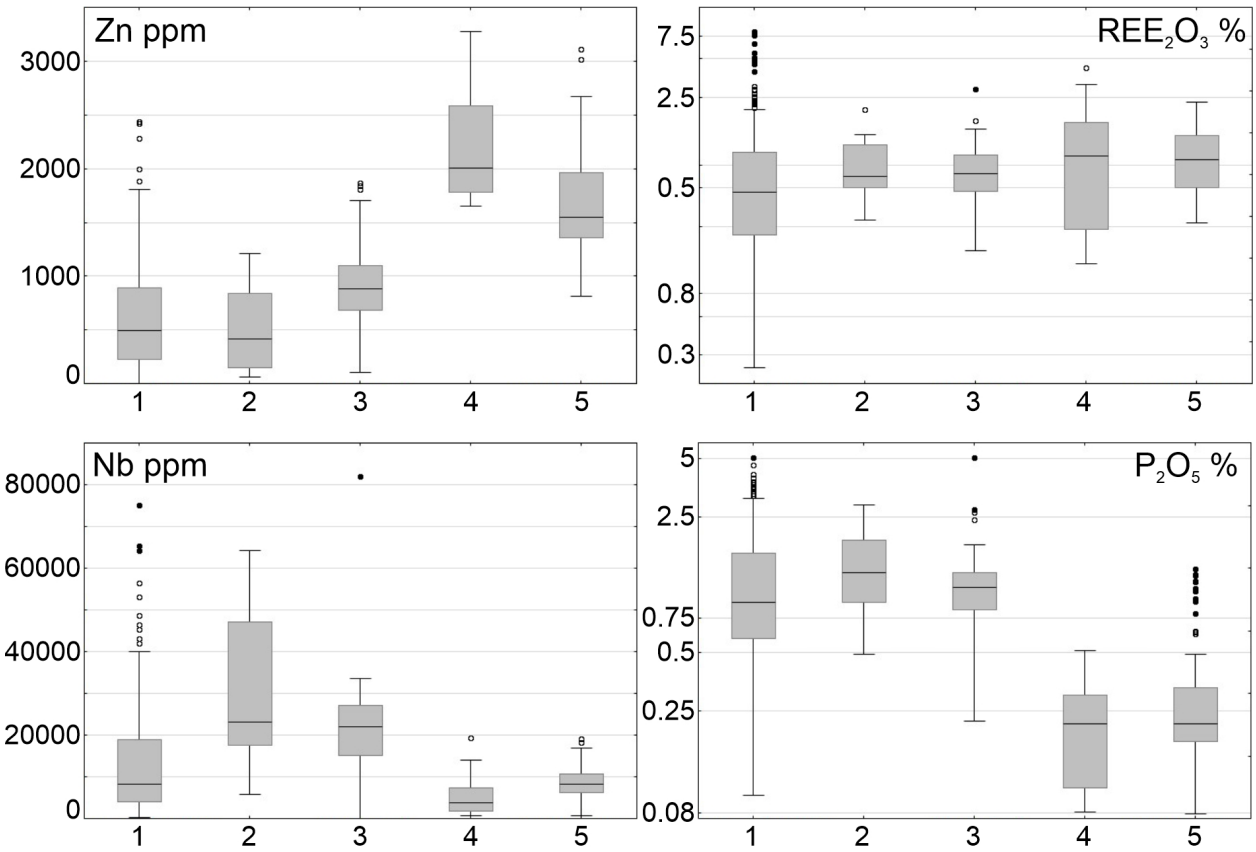

1: Lateritic crust (in surface); 2: Lateritic crust (in surface restricted to the area under influence of drill holes); 3: Lateritic crust (in drill holes); 4: Manganesiferous crust; 5: Siderite carbonatite.

Figure 12. Boxplots comparing the grades between soil grid and drill holes SL-04 and UA-01 to UA-04 samples for different lithologies. Open and closed circles represent outlier and extreme outlier values, respectively.

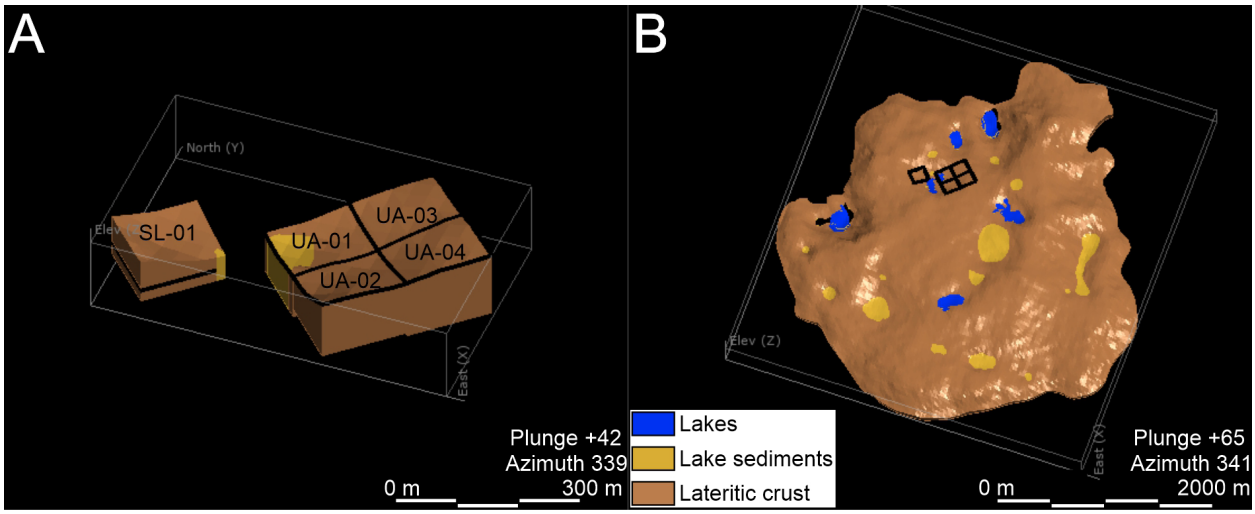

Figure 13. (A) Perspective view of the geological model sectioned at RSL = 165 m. (B) Detailed perspective view with the 5 blocks constructed around the drill holes that compose Domain 1.

DISCUSSION ON THE EXPLORATION POTENTIAL OF SLCC

Carbonatite complexes are characteristically composed of several magmatic pulses resulting in a complex variety of rock types with different chemical and modal compositions (Mitchell 2015). Therefore, it is difficult to produce accurate geological maps or to even trace correlations between adjacent drill holes. Despite these difficulties, the attempt to produce a new geological map of the MSL proved worthwhile since the modifications that were introduced, mainly the incorporation of additional areas of lateritic crust, have a significant impact on the modeling and, consequently, in the estimation of Nb and REE tonnages in the lateritic crust and lake sediments.

The different RSL at which the carbonatites were intersected in drill holes SL-02 and SL-04 and the depths of all five holes, drilled entirely within the lateritic crust, reflect the irregular nature of the carbonatite's upper boundary, represented by a lobated shape in the geological model (Figs. 9B

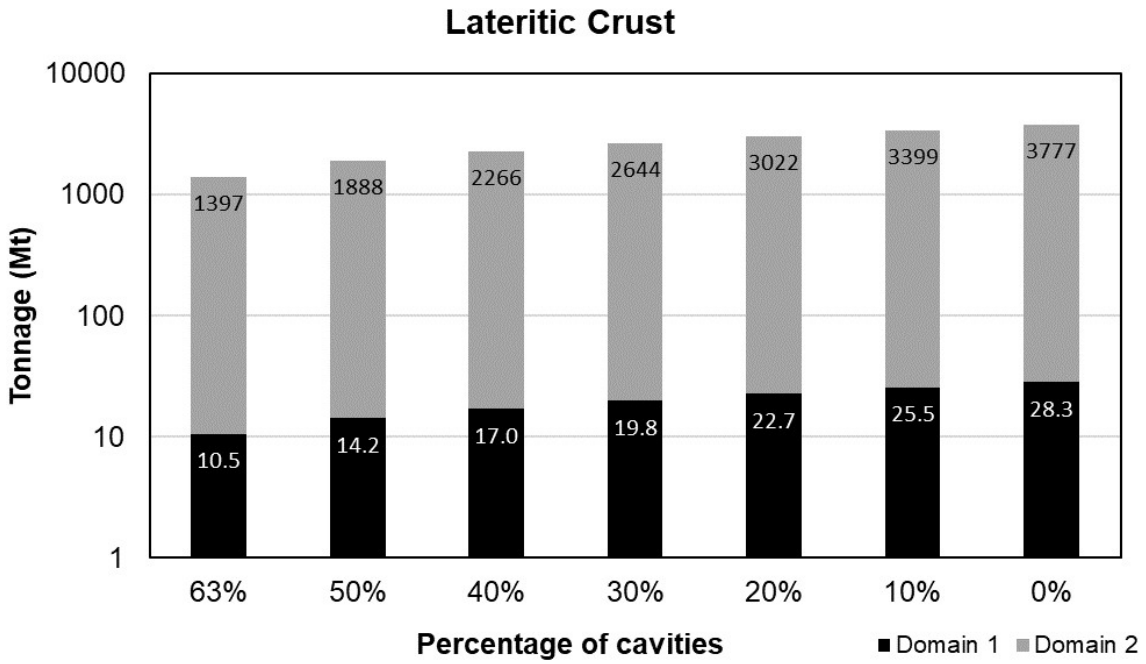

Figure 14. Scenarios of lateritic crust tonnage in Domains 1 and 2 according to hypothetical percentages of cavities in MSL. Logarithmic scale is applied on Y axis. Percentage of cavities are referred to as the percentage of open spaces that cause poor core recovery, and not the natural pores of the lateritic crust.

Table 4. Representative average grades for Domains 1 and 2.

	Ton (Mt)	Nb_2O_5 (%)	TiO_2 (%)	Sn (ppm)	W (ppm)	P_2O_5 (%)	REE_2O_3 (%)
Domain 1*							
SL-01	3.95	1.89	3.43	62	272	0.74	0.78
UA-01	4.50	3.34	4.68	101	542	1.62	0.77
UA-02	6.44	3.95	5.50	117	573	1.05	0.70
UA-03	5.45	2.47	3.38	70	322	0.44	0.34
UA-04	7.98	2.84	4.88	95	399	1.29	0.91
Total	**28.3**	**2.97**	**4.50**	**91**	**429**	**1.05**	**0.71**
Domain 2**							
Soil grid	-	**1.17**	**1.94**	**64**	**143**	**0.91**	**0.46**
Soil grid in the area of influence of the drill holes	-	**3.30**	**6.91**	**125**	**784**	**1.29**	**0.61**

and 9C). This is explained by the fluidal nature of the intrusion that can easily occupy structural discontinuities or by the irregular weathering depths.

Although there is a lack of geological information that could lead to the construction of a more implicit model, it has satisfactorily fulfilled its function as an auxiliary tool to display the relative position of the geological units in the surface and subsurface and consequently served as the basis to estimate volumes.

The complex lithological distribution within carbonatite complexes may also explain some contrasting geochemical patterns obtained in the soil grids over the SLCC. The distinctly higher Nb grades over MSL relative to MM and MN and the opposite trend for REE and P_2O_5 grades (Fig. 10), coupled with other geochemical heterogeneities may indicate distinct carbonatite protoliths coupled with different weathering conditions. These characteristics may be responsible by diverse degrees of geochemical concentration or leaching among the three hills. For instance, the Fe_2O_3 concentration is greater in MSL and MN in comparison to MM. This may indicate a lower degree of laterization in the latter, which on its turn may reflect a carbonatite with less iron.

The strong correlation among Nb, TiO_2, Sn and W (> 0.75) (Tab. 3) in the lateritic crust of the soil grid is typically an immobile metal association that seems to have been inherited from the lateritic crusts at depth as observed in the drill holes (Fig. 3). Similarly, the high correlation between REE, P_2O_5 and Al_2O_3 (Tab. 3) indicates that REE occur in phosphates like florencite-(Ce) (Giovannini *et al.* 2017) in the lateritic crust. These metals tend to concentrate near the center of the MSL, bordering the Esperança Basin (Fig. 11). This may point to the past existence of a drainage network that contributed

to the leaching of P_2O_5 and REE from the lateritic crust and consequent florencite mineralization in the sediments that filled the Esperança Basin.

Exploration potential of the lateritic crust

Domain 1's lateritic crust is estimated to contain between 10.5 Mt and 28.3 Mt, depending on the volume of cavities, with 2.97 wt% Nb_2O_5 and 0.71 wt% REE_2O_3. Domain 2 is estimated to contain between 1.40 Bt and 3.78 Bt with 1.17 wt% Nb_2O_5 and 0.46 wt% REE_2O_3. Domain 1 may be compared to the Justo (1983)'s Measured Reserves, estimated to contain 38.4 Mt of ore with a grade of 2.85 wt% Nb_2O_5 based on drill holes UA-01 to UA-04, while Domain 2 may be compared to the Indicated plus Inferred Reserves, estimated to contain 2.86 Bt of ore with a grade close to 2.80 wt% Nb_2O_5 (Tab. 1).

Similar parameters to Justo (1983)'s were used to calculate Domain 1's tonnage such as the size of the area of influence of drill holes and density. However, Domain 1 also included the grade and tonnage of drill hole SL-01 and the base of its volume is restricted to the depth where each of the five drill holes could be continually sampled (RSL = 206 m for SL-01 and RSL = 197 m for UA-01 to UA-04). Justo (1983) considered the 47 m extension below the base of each of the four UA drill holes (RSL = 150 m) as part of the Measured Reserve (Fig. 2).

The Nb_2O_5 grades were obtained from a database where the quality of the analytical results produced by the SGS-Geosol Lab was properly controlled and found to be approximately 8% higher than the analytical results produced by the LAMIN Lab for the Uaupés Project (Fig. 7). In addition, the grade estimates for Domain 1 did not include the generally Nb-poor intervals of the manganesiferous crust.

Although the Indicated plus Measured Reserves estimated by Justo (1983) falls within the range of 1.40-3.78 Bt estimated for the Domain 2's lateritic crust, the parameters and methods applied are significantly different, especially considering the upper and lower RSL adopted for the boundaries. While Justo (1983) considered the entire MSL volume between RSL = 195 and 305 m (Fig. 2) as lateritic crust, in this work a thicker volume is considered between RSL = 165 m and the surface (Figs. 9B and 9C). In addition, through the geological model it was possible to subtract the volume of lake sediments and manganesiferous crust. It should also be noted that according to the core description of drill hole SL-01 by Viegas Filho and Bonow (1976), lateritic crusts occur at least down to RSL = 10 m (Fig. 2), pointing to a substantial ore tonnage increase.

The Nb grades of the lateritic crust from the soil grid under the area of influence of drill holes UA-01 to UA-04 and SL-01 are greater than the the remaining grid (Tab. 4). This directly reflects the higher Nb grades observed in these drill holes regardless of the surficial grade enrichment (Fig. 3). These results suggest that the average grade of 2.81 wt% Nb_2O_5 found by Justo (1983) for the Indicated and Inferred reserves of MSL is overestimated as his calculations were based only on drill holes UA-01 to UA-04 that covered a particularly Nb-rich portion of the grid area. Due to these reasons, in this work, the Nb grade estimated for Domain 2 is based on the median grade of the grid outside Domain 1. The result is 1.17 wt% Nb_2O_5, however, considering that the grade of the lateritic crust is consistently enriched in about 5 to 10% near the surface (reworked lateritic crusts), the median grade for the lateritic crust in Domain 2 may be recalculated to be close to 1.10 wt% Nb_2O_5. Despite this preliminary grade estimation being based only on surface samples, it may be argued that there is in fact a direct comparison between the surface and drill hole grades. As a consequence, the surface soil grid Nb anomaly detected in the area immediately to the east of Domain 1 (Fig. 11) may indicate the presence of additional high grade Nb tonnage. This should be further investigated and, if confirmed, it can significantly impact the whole potential of MSL.

Different scenarios have been created considering the volume of cavities and how this impacts the tonnage estimate of the mineralized lateritic crusts in Domains 1 and 2. These tonnages are plotted in a global context (Fig. 15) where it becomes apparent that for both domains the grades and tonnages are globally relevant even in the worst-case scenario.

Based on the various uncertainties inherent to the MSL deposit, mainly the low core recovery, the imprecise georeferencing and the limited amount of drilling conducted in the area, it is proposed that the Domains 1 and 2 of the MSL lateritic crust deposit be classified as "Results of Exploration". This term is generically applied to a mineralized body that does not have sufficient exploration data and, therefore, its resources cannot be estimated or classified (CBRR, 2016). Instead, according to the guide, the exploration results are expressed in terms of a range of grade and tonnage.

The MSL Nb deposit is typically defined as supergene and comparable to other Brazilian examples such as Araxá (Minas Gerais) and Catalão I and II (Goiás) where the grades vary between 1.08 and 2.48 wt% Nb_2O_5. Mitchell (2015) mentions other similar Nb deposits hosted in laterites such as Lueshe and Bingo (Congo), Mabounié (Gabon), Sukulu (Uganda) and Mt. Weld (Australia) whose grades and tonnages are given in Fig. 15 where it becomes clear how outstanding the grades present in the MSL deposit are. However, in most of these deposits, the main ore mineral is pyrochlore, while the Nb in MSL is hosted mainly in Nb-rich rutile and/or brookite and, secondarily, in goethite (Giovannini *et al.* 2020). It is also singular that the MSL deposit derived from the lateritic weathering of a siderite carbonatite which, due to its high Fe content coupled with its exposure to a humid tropical climate, led to the development of such a thick lateritic crust.

Significant grades of other potentially economic metals such as Ti-Sn-W that are contained in the Nb-rich rutile's structure and could potentially be considered a subproduct were detected. For example, TiO_2 grades are as high as 4.5 wt% in Domain 1 and 1.94 wt% in Domain 2 (Tab. 4).

The lateritic crust of MSL also contains REE mineralization in the form of cerianite and florencite-(Ce), and, to a lesser extent, Fe oxy-hydroxides (Giovannini e*t al.* 2017). Domains 1 and 2 contain REE grades of 0.71 wt% and 0.46 wt% REE_2O_3, respectively. These grades are low compared to the lateritic REE deposits of Araxá, where the reported reserves in two areas in 2016 were of 13.36 Mt @ 3.02 wt% and 6.52 Mt @

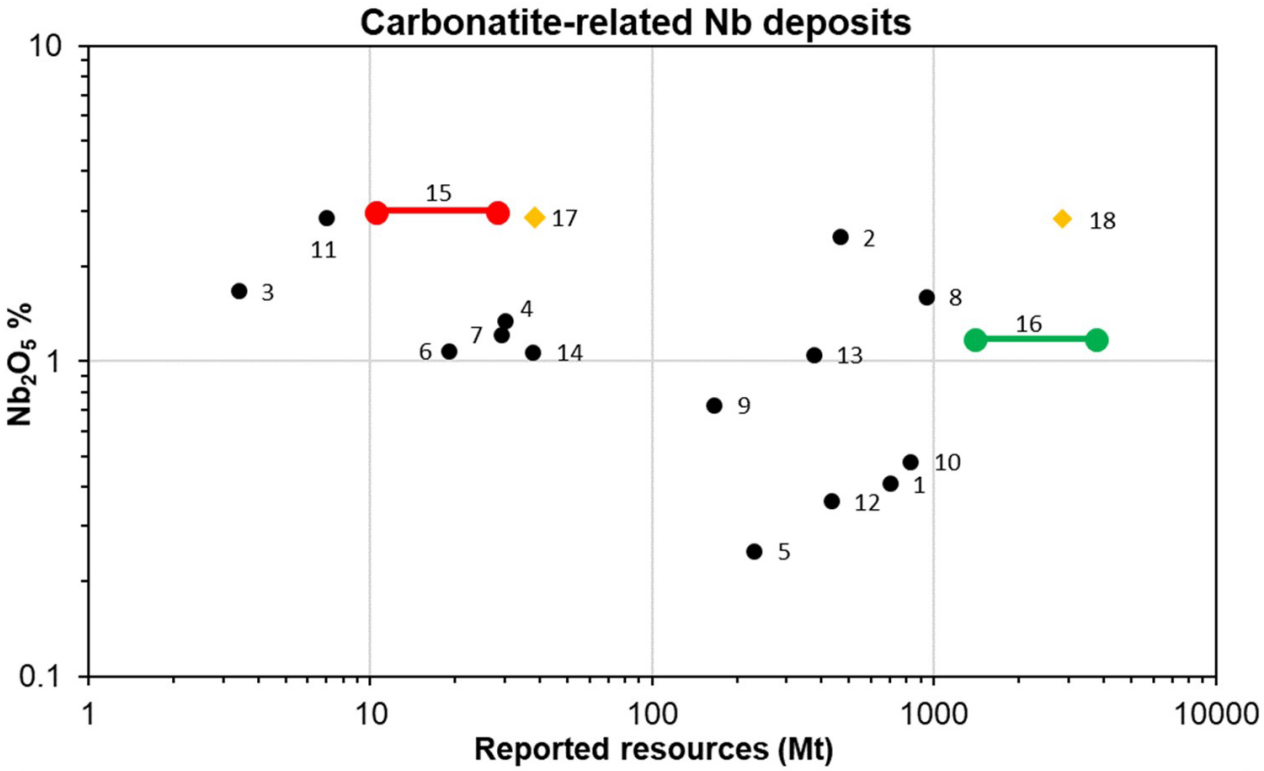

#	Complex	Country	Type	Status	Resources	Tonnage (Mt)	Nb_2O_5 (%)	References
1	St-Honoré	Canada	Primary	Active Mine	Measured, Indicated and Inferred	697.6	0.41	IAMGOLD (2013)
2	Araxá	Brazil	Residual	Active Mine	-	462.0	2.48	Carneiro (2016)
3	Catalão II	Brazil	Residual	Active Mine	Probable reserve	3.4	1.67	Cordeiro et al. (2011)
4	Lueshe	Congo	Residual	Past producer	-	30.0	1.34	Deans (1966)
5	Sukulu	Uganda	Residual	Past producer	-	230.0	0.25	Deans (1966); van Straaten (2002)
6	Catalão I	Brazil	Residual	Past producer	-	19.0	1.08	Cordeiro et al. (2011)
7	Catalão I	Brazil	Primary	Resource	Measured and Indicated	29.0	1.22	Cordeiro et al. (2011)
8	Araxá	Brazil	Primary	Resource	-	940.0	1.60	Carneiro (2016)
9	Tapira	Brazil	Residual	Resource	-	166.0	0.73	Mariano (1989); Biondi (2005)
10	Bonga	Angola	Primary	Resource	-	824.0	0.48	Pena (1989)
11	Bingo	Congo	Residual	Resource	-	7.0	2.86	Woolley (2001)
12	Aley	Canada	Primary	Resource	Measured, Indicated and Inferred	430.0	0.36	Simpson (2012)
13	Mabounié	Gabon	Residual	Resource	Measured and Indicated	374.0	1.05	Chakhmouradian et al. (2015)
14	Mt. Weld	Australia	Residual	Resource	Indicated and Inferred	37.7	1.07	Lynas Corp. (2019)
15	MSL Domain 1	Brazil	Residual	Resource	Exploration results	10.5 - 28.3	2.97	This work
16	MSL Domain 2	Brazil	Residual	Resource	Exploration results	1400 - 3780	1.17	This work
17	MSL by Justo (1983)	Brazil	Residual	Resource	Measured	38.4	2.85	Justo (1983)
18	MSL by Justo (1983)	Brazil	Residual	Resource	Indicated and Inferred	2859.5	2.81	Justo (1983)

Figure 15. Grade and tonnage of carbonatite-related Nb deposits. Green and red highlight Domains 1 and 2, while yellow highlights calculations made by Justo (1983). Logarithmic scale is applied.

2.30 wt% REE_2O_3 respectively (Costa *et al.* 2019). According to the authors, more recently measured reserves of 44 Mt @ 1.41 wt% were approved for this area. At Mt. Weld, the strongest REE enrichment coincides with the presence of Al-phosphate in the supergene zone of the deposit (Lottermoser 1990) that contains total resources of 55.2 Mt @ 5.4 wt% REE_2O_3

considering a cutoff of 2.5 wt% REE_2O_3 (Lynas Corp. 2019). The Ngualla deposit in Tanzania is hosted in weathered carbonatite and contains 21.3 Mt @ 4.75 REE_2O_3 (Witt *et al*. 2019). However, the competitivity of these REE supergene deposits still needs to be verified (Chakhmouradian and Zaitsev, 2012). In the national context, the Serra Verde deposit was recently discovered, containing 300 Mt @ 0.15 wt% REE_2O_3 + Y in ionic clays (Costa *et al*. 2019).

The proportion of each REE, in the composition of the average REE grade of each unit studied in this work, is shown in Tab. 5. A clear dominance of La and Ce is observed in general. In the case of the manganesiferous crust, Ce proportion is outstanding. REE mineralization in carbonatites are knowingly dominated by LREE (Chakhmouradian and Wall 2012) as confirmed in the case of SLCC and its lateritic products.

Scandium is another potentially economic metal in the SLCC. In drill hole SL-01, the Sc composite grade across the entire 58.75 m long hole is 183 ppm. This is lower than the grades of the Australian Sc laterite deposits of Syerston (21.7 Mt @ 429 ppm Sc) and Nyngan (12 Mt @ 261 ppm Sc) reported by Williams-Jones and Vasyukova (2018). According to Verplanck (2017), the greatest Sc enrichment occurs in lateritic crusts developed over Sc enriched protoliths.

Manganesiferous crusts, with high grades of REE, and Zn were detected in drill holes SL-01 and UA-03 on intervals at 9.5 and 22.8 m thick, respectively. Cerium is distinctly enriched (Tab. 5) due to the abundance of cerianite (Giovannini *et al*. 2017). In drill hole SL-01, the composite grades over a 9.4 m thick interval are 25.4 wt% MnO, 1.58 wt% REE_2O_3 and 2264 ppm Zn. In drill hole UA-03, the composite grades over a 22.8 m thick interval are 4.11 wt% MnO, 0.21 wt% REE_2O_3 and 1977 ppm Zn. Considering these two intersections combined, the composite grades are 10.3 wt% MnO, 0.61 wt% REE_2O_3 and 2061 ppm Zn.

Exploration potential of the carbonatite

High Nb grades were detected in the "border siderite carbonatite", with one core sample grading 2.72 wt% Nb_2O_5 near the end of drill hole SL-02. Drill hole SL-04 intersected "core siderite carbonatite" and "REE-rich core siderite carbonatite" between 233.65 and 493 m with a composite grade of 1.27 wt%. Compared to Araxá, where the average grade of the primary deposit is 1.6 wt% Nb_2O_5 and Catalão-I (1.22 wt% Nb_2O_5). These grades of siderite carbonatite are relevant.

Significant REE grades are found across all intersected siderite carbonatites in drill hole SL-04, but it is particularly enriched in the "REE-rich core siderite carbonatite", where the composite grade is 1.45 wt% REE_2O_3. This grade is comparable to others such as the Canadian deposits of Nechalacho (88 Mt @ 1.53 wt% REE_2O_3) and Strange Lake (66 Mt @ 1.52 wt% REE_2O_3) but is considerably lower if compared to the largest producers, Bayan Obo (135 Mt @ 6 wt% REE_2O_3) (Williams-Jones *et al*. 2012) or Mountain Pass (16.7 Mt @ 7.98 wt% REE_2O_3) (Mariano and Mariano Jr. 2012).

Scandium is another important metal occurring in the siderite carbonatite with a median grade of 517 ppm. However, considering the 179 m thick interval between 314-493 m in drill hole SL-04, the composite grade reaches 604 ppm Sc, which is an extremely high grade compared to most mineable Sc deposits (Williams-Jones and Vasyukova 2018). In the carbonatite of Bayan Obo, Sc is extracted as a subproduct of the REE ore, with a grade of 200 ppm (Li *et al*. 2013). The apparent Sc depletion in the lateritic crust, where the composite grade in drill hole SL-01 is 183 ppm, may be reflecting a weathering environment that promotes Sc leaching but it may also reflect a particular Sc enriched siderite carbonatite intersected in drill hole SL-04. In this case, the comparison with the lateritic crust above would not be valid. However, a more challenging and equally possible alternative is that the typical Sc enriched lateritic crust was not detected by the scarce drilling performed so far, especially in the lower portion of the crust. Nevertheless, Sc enrichment zones may occur similarly to HREE, which is preferentially leached in comparison to LREE from the upper portion of the lateritic crust.

Exploration potential of the lake sediments

The tonnage of REE mineralized lake sediments from the Esperança Basin have been estimated by Bonow and Issler (1980) as 7.8 Mt. In the current work, this has been estimated as 11.8 Mt based on the clay sediments enriched in REE and P_2O_5 intersected by the drill hole SL-04 from surface down

Table 5. Individual proportion of REE per lithology.

	Lake Sediments (SL-04 00.00-71.90 m)	Lateritic Crust (Domain 1)	Lateritic Crust (Domain 2)	Mn Crust	REE-rich core siderite carbonatite
REE_2O_3 grade	1.76%	0.71%	0.46%	0.61%	1.45%
La	23.4%	20.6%	22.8%	5.4%	19.3%
Ce	45.1%	52.2%	50.8%	81.3%	40.5%
Pr	4.7%	4.8%	5.0%	1.3%	4.7%
Nd	19.5%	12.8%	14.4%	3.9%	19.3%
Sm	3.3%	2.0%	2.4%	1.2%	6.3%
Eu	0.6%	0.6%	0.6%	0.4%	1.6%
ETRP	1.9%	3.1%	2.1%	2.6%	4.3%
Y	1.5%	3.8%	2.1%	3.9%	4.0%
Total	100%	100%	100%	100%	100%

to 71.90 m. This tonnage difference mainly occurs due to the fact that Bonow and Issler (1980) excluded the first 14.65 m from their calculations, which was considered as capping. The REE and phosphate likely occur associated in the form of florencite-(Ce) that has been identified by Giovannini *et al.* (2017). Another reason is the model adopted for the geometry of the karst filled by the sediments. While Bonow and Issler (1980) adopted the inverted cone model, this work adopted a cylindrical shape which is simpler and likely more realistic given a scenario where no in depth information is available on the actual geometry of these karst cavities.

The REE grade estimated by Bonow and Issler (1980) for the Esperança Basin was 1.5 wt% REE_2O_3 based on individual cores samples. An estimated grade of 1.76 wt% REE_2O_3 is proposed by this study based on more representative continuous core samples.

It is also worth emphasizing the importance that all the other depressions present at MSL must increase the potential resources of the mineralized lake sediments. In the geological model produced by this work, it has been speculated that all depressions were similarly filled by sediments.

Considering some important world REE deposits it is clear that the grade and tonnage at Esperança Basin are considerably smaller. However, in favor of this deposit, it should be noted that the potential REE ore is hosted by a poorly consolidated material which may be favorable to its mining and processing.

CONCLUSION

An up-to-date scenario of the exploration so far conducted in SLCC has been presented. This included a compilation of information from the past exploration programs carried out in the area and new estimations for grade and tonnage of Nb and other important metals such as REE, Sc, Zn in the lateritic crust, siderite carbonatites and lake sediments. This was made possible due to the new sampling and chemical analyses performed on the archived drill cores and pulps.

The quality control conducted on the new analytical data by the SGS-Geosol lab revealed an analytical precision of 2.99% for Nb and generally better than 10% for most other metals, including REE. The Nb results produced by the SGS Geosol Lab are close to 8% higher than those previously produced by the LAMIN/CPRM lab on the same drill hole pulps. This difference has a significant impact on the average Nb grade of the deposit.

The new geological map produced for the MSL area allowed for constructing a 3D geological model that incorporates additional tonnages of mineralized lateritic crust, which was segmented in two. Domain 1, which contains five drill holes located on the most Nb-enriched portion of MSL, was estimated to contain between 10.5 to 28.3 Mt at 2.97 wt% Nb_2O_5 and 0.71 wt% REE_2O_3. Domain 2, where no holes have been drilled, contains an estimated tonnage of lateritic crust between 1.40 Bt and 3.78 Bt. The grades were estimated as the median values of the prospective grid over the lateritic crust in Domain 2 as 1.17 wt% Nb_2O_5 and 0.46 wt% REE_2O_3.

The different tonnage scenarios proposed is a function of the percentage of cavities present in the lateritic crust. This feature greatly impacts the tonnage of lateritic crust, but it remains an unknown parameter since the low drilling recovery does not allow differentiating between cavities and poor drilling performance. This fact along with other uncertainties, mainly derived from the low amount of drilling and imprecise locations, led to propose the grade and tonnage estimates for MSL in this work to be classified as "Results of Exploration", which is believed to be more in accordance with present resources classification concepts considering the actual geological knowledge on the deposits.

A summary of the potential exploration targets identified in this work are summarized in Tab. 6. High Sc grades were

Table 6. Summary of the main mineralizations detected in MSL.

Classification	Lithology	Local	Tonnage	Nb_2O_5 (%)	TiO_2 (%)	Sn (ppm)	W (ppm)	REE_2O_3 (%)	P_2O_5 (%)	Sc (ppm)	Zn (ppm)	MnO (%)
Exploration results	Lateritic crust	Domain 1	10.5 to 28.3 Mt	2.97	4.5	91	429	0.71	1.05	183	-	-
		Domain 2	1.40 to 3.78 Bt	1.17	1.94	64	143	0.46	0.91	-	-	-
	Lake sediments	SL-04 (0.00-71.90 m)	11.8 Mt	-	-	-	-	1.76	2.36	-	-	-
Enriched interval	Manganesiferous crust	SL-01 (30.40-39.90 m) & UA-03 (75.20-98.00 m)	-	-	-	-	-	0.61	-	-	2061	10.3
	"Border siderite carbonatite"	SL-02 (221.60-227.70 m)	-	2.72	2.76	-	-	2.33	1.3	-	3381	-
	"Core siderite carbonatite" and "REE-rich core siderite carbonatite"	SL-04 (314.00-493.00 m)	-	-	-	-	-	-	-	604	-	-
		SL-04 (233.65-493.00 m)	-	1.27	-	-	-	-	-	-	-	-
		SL-04 (238.00-297.00 m)	-	-	-	-	-	-	-	-	2356	-
		SL-04 (288.00-340.00 m)	-	-	-	-	-	1.45	-	-	-	-

detected in the lateritic crust (183 ppm Sc), which is comparable to other supergene Sc deposits. In addition, in the drill hole SL-04's carbonatites, high Sc grades were detected (604 ppm over 179 m). These data may lead to new possibilities for Sc exploration in the MSL area.

The Esperança Basin's lake sediments were also identified as containing possible resources estimated as 11.8 Mt at 1.76 wt% REE_2O_3 and 2.36 wt% P_2O_5. In addition, it is possible that the other depressions present in the MSL are similarly mineralized.

The manganesiferous crust may also constitute another exploration target as they contain anomalous grades for Zn and REE, with a high proportion of Ce.

The siderite carbonatites also showed high Nb grades (1.27 to 2.72 wt% Nb_2O_5). Similarly to the Araxá and Catalão's deposits in Brazil, this primary portion of the deposit may contribute to its economic potential. Apart from Nb, high grades of REE (1.45 to 2.33 REE_2O_3); Sc (831 ppm); Zn (2,381 to 2,356 ppm) have also been detected in the siderite carbonatites.

The amount of exploration works necessary to better estimate the resource potential of the MSL is immense. Apart from additional drilling, the estimation of the cavity volumes is also particularly relevant, as well as more accurate density tests, the use of geophysical methods to estimate the volume of cavities and the acquisition of more accurate topographic data (e.g., LiDAR method). It was possible to demonstrate that Nb anomalies on the soil grid is an effective way to understand the underlying mineralization despite the geochemical enrichment in the upper reworked lateritic crust. This raises confidence to recommend a program of regular soil sampling all over the MSL's surface as well as the other hills (MM and MN), which despite not showing a similar Nb anomaly pattern to MSL, have shown REE and P_2O_5 anomalies. This could reveal other important targets such as the one located immediately to the east of Domain 1, where the potential for addition high grade Nb resources is indeed very large.

ACKNOWLEDGEMENTS

The current work was executed with the support of "Coordenação de Aperfeiçoamento de Pessoal de Nível Superior – Brasil" (CAPES) in the form of an MSc scholarship. We would like to thank the Brazilian Geological Survey (CPRM) for the incentive to develop this work and for providing the data that made it possible. SGS-Geosol is also thanked for providing guidance on the procedures for quality control of the geochemical analyses.

ARTICLE INFORMATION

Manuscript ID: 20210031. Received on: 21 APR 2021. Approved on: 20 NOV 2021.

How to cite this article: Bento J.P.P., Porto C.G., Takehara L., Silva F.J., Bastos Neto A.C., Machado M.L., Duarte A.C. Mineral potential re-evaluation of the Seis Lagos Carbonatite Complex, Amazon, Brazil. *Brazilian Journal of Geology*, 52(1):e20210031, 2022. https://doi.org/10.1590/2317-4889202120210031.

J.P.B. was involved in producing and writing all parts of the article, which was the final product of his MSc. Thesis; C.P. was involved in supervising all of the work and also defining the scope and structure of the research; F.S. provided great contributions on the statistical parts of the results and discussions; M.M. directly contributed with the production of Figs. 1, 2 and 8, and revision of the manuscript; A.C.D., who is also developing a MSc. Thesis about the same area, wrote the "Sampling and geochemical analyses" section and also constantly shared information and data; A.N. revised and improved the manuscript; L.T., representing the Brazilian Geological Survey, provided all the geochemistry data and also revised the manuscript.

Competing Interests: The authors declare no competing interests.

REFERENCES

Berger V.I., Singer D.A., Orris G.J. 2009. Carbonatites of the world, explored deposits of Nb and REE—database and grade and tonnage models. *U.S. Geological Survey Open-File Report 2009-1139*, 17 p.

Biondi J.C. 2005. Brazilian mineral deposits associated with alkaline and alkaline-carbonatite complexes. *In*: Comin-Chiaramonti P., Gomes C.B. (Eds.). *Mesozoic to Cenozoic alkaline magmatism in the Brazilian Platform*. São Paulo: Editora da Universidade de São Paulo, Fapesp, p. 707-750.

Bonow C.W., Issler R.S. 1980. Reavaliação e aspectos econômicos do jazimento de terras raras e ferro-ligas do Lago Esperança Complexo Carbonatítico dos Seis Lagos - Amazonas - Brasil. *In*: Congresso Brasileiro de Geologia, Balneário de Camboriú, 31., 1980. *Annals*... p. 1431.

Carneiro T. 2016. Potencial Mineral do Brasil: Nióbio – desenvolvimento tecnológico e liderança. *In*: Melfi A.J., Misi A., Campos D.A., Cordani U.G. (Eds.). *Recursos Minerais no Brasil*. Academia Brasileira de Ciências, p. 60-67.

Chakhmouradian A.R., Reguir E.P., Kressall R.D., Crozier J., Pisiak L.K., Sidhu R., Yang P. 2015. Carbonatite-hosted niobium deposit at Aley, northern British Columbia (Canada): mineralogy, geochemistry and petrogenesis. *Ore Geology Reviews*, **64**:642-666. https://doi.org/10.1016/j.oregeorev.2014.04.020

Chakhmouradian A.R., Wall F. 2012. Rare Earth elements: minerals, mines, magnets (and more). *Elements*, **8**(5):333-340. https://doi.org/10.2113/gselements.8.5.333

Chakhmouradian A.R., Zaitsev A.N. 2012. Rare Earth mineralization in igneous rocks: sources and processes. *Elements*, **8**(5):347-353. https://doi.org/10.2113/gselements.8.5.347

Comissão Brasileira de Recursos e Reservas (CBRR). 2016. *Guia CBRR para Declaração de Resultados de Exploração, Recursos e Reservas Minerais*. CBRR. Available on: http://cbrr.org.br/docs/guia_declaracao.pdf. Accessed on: Apr 30, 2019.

Cordeiro O.C.G., Brod J.A., Palmieri M., Oliveira C.G., Barbosa E.S.R., Santos R.V., Gaspar J.C., Assis L.C. 2011. The Catalão I niobium deposit, central Brazil: resources, geology and pyrochlore chemistry. *Ore Geology Reviews*, **41**(1):112-121. https://doi.org/10.1016/j.oregeorev.2011.06.013

Cordeiro R.C., Turcq B., Moreira L.S., Rodrigues R.A.R., Simões Filho F.F.L., Martins G.S., Santos A.B., Barbosa M., Conceição M.C.G., Rodrigues R.C., Evangelista H., Moreira-Turcq P., Penido Y.P., Sifeddine A., Seoane J.C.S. 2014. Palaeofires in Amazon: Interplay between land use change and palaeoclimatic events. *Palaeogeography, Palaeoclimatology, Palaeoecology*, **415**:137-151. http://dx.doi.org/10.1016/j.palaeo.2014.07.020

Costa M.L., Fonseca L.R., Angélica R.S., Lemos V.P., Lemos R.L. 1991. Geochemical exploration of the Maicuru alkaline-ultramafic-carbonatite complex, northern Brazil. *Journal of Geochemical Exploration*, **40**(1-3):193-204. https://doi.org/10.1016/0375-6742(91)90038-V

Costa M.M.D., Medeiros K.A., Lima T.M. 2019. *Sumário Mineral 2017*. Brasília: ANM, 201 p.

Cowan E.J., Beato R.K., Ross H.J., Fright W.R., Mclennan T.J., Evans T.R., Carr J.C., Lane R.G., Bright D.V., Gillman A.J., Oshust P.A., Titley M. 2003. Practical Implicit Geological Modelling. *In*: AUSIMM 5th International Mining Geology Conference, 17, 2003. *Conference Paper…* Bendigo, Victoria, p. 89-99.

Deans T. 1966. Economic geology of African carbonatites. *In*: Tuttle O.F., Gittins J. (Eds.). *Carbonatites*. New York: Wiley, p. 385-413.

Freyssinet P., Butt C.R.M., Morris R.C., Piantone P. 2005. Ore-forming processes related to lateritic weathering. *Economic Geology 100th Anniversary Volume*, **100**:681-722. https://doi.org/10.5382/AV100.21

Giovannini A.L., Bastos Neto A.C., Porto C.G., Pereira V.P., Takehara L., Barbanson L., Bastos P.H.S. 2017. Mineralogy and geochemistry of laterites from the Morro dos Seis Lagos Nb (Ti, REE) deposit (Amazonas, Brazil). *Ore Geology Reviews*, **88**:461-480. https://doi.org/10.1016/j.oregeorev.2017.05.008

Giovannini A.L., Mitchell R.H., Bastos Neto A.C., Moura C.A.V., Pereira V.P., Porto C.G. 2020. Mineralogy and geochemistry of the Morro dos Seis Lagos siderite carbonatite, Amazonas, Brazil. *Lithos*, **360-361**:105433. https://doi.org/10.1016/j.lithos.2020.105433

IAMGOLD. 2013. *NI 43-101 Technical Report, Update on Niobec Expansion, December 2013*. IAMGOLD. Available on: https://miningdataonline.com/reports/Niobec_12102013_TR.pdf. Accessed on: Jul 15, 2020.

Justo L.J.E.C. 1983. *Projeto Uaupés:* relatório final de pesquisa. [Alvarás n. 2702, 2844/81]. Manaus: CPRM. Available on: http://rigeo.cprm.gov.br/jspui/handle/doc/7956?mode=full. Accessed on: Apr 30, 2019.

Kynicky J., Smith M.P., Xu C. 2012. Diversity of rare Earth deposits: the key example of China. *Elements*, **8**(5):361-367. https://doi.org/10.2113/gselements.8.5.361

Le Maitre R.W. 2002. *Igneous rocks:* a classification and glossary of terms. Cambridge: Cambridge University Press, 256 p.

Li M., Hu D., Liu Z., Zhang D., Gao K., Chen Y. 2013. Leaching technology of scandium in Bayan Obo tailings. *Journal of the Chinese Society of Rare Earths*, **31**:703-708.

Lottermoser B.G. 1990. Rare-earth element mineralisation within the Mt. Weld carbonatite laterite, Western Australia. *Lithos*, **24**(2) https://doi.org/10.1016/0024-4937(90)90022-S:151-167.

Lynas Corp. 2019. *2019 Annual Report*. Lynas Corporation Ltd. Available on: https://www.lynascorp.com/wp-content/uploads/2019/10/191002-Annual-Report-Appendix-4G-and-Corporate-Governance-Statement-1979978-1.pdf. Accessed on: Jul. 15, 2020.

Mariano A.N. 1989. Nature of economic mineralization in carbonatites and related rocks. *In*: Bell K. (Ed.). *Carbonatites*. London, Unwin Hyman, p. 149-176.

Mariano A.N., Mariano Jr. A. 2012. Rare Earth mining and exploration in North America. *Elements*, **8**(5):369-376. https://doi.org/10.2113/gselements.8.5.369

Mitchell R.H. 2015. Primary and secondary niobium mineral deposits associated with carbonatites. *Ore Geology Reviews*, **64**(1):626-641. https://doi.org/10.1016/j.oregeorev.2014.03.010

Nahon D., Tardy Y. 1992. The Ferruginous Laterites. *In*: Butt C.R.M., Zeegers H. (Eds.). *Handbook of Exploration Geochemistry*. Amsterdã: Elsevier Science, p. 41-55.

Pena F.M. 1989. Perfil analítico do pirocloro (nióbio). Departamento Nacional da Produção Mineral, **18**,1-59 p. Boletim.

Pinheiro S. da S., Fernandes P.E.C.A., Pereira E.R., Vasconcelos E.G., Pinto A. do C., Montalvão R.M.G., Issler R.S., Dall'Agnol R., Teixera W., Fernandes C.A.C. 1976. Geologia. *In*: Projeto RADAMBRASIL – levantamento de recursos naturais. v. 11. Folha NA-19 Pico da Neblina, 369 p.

Rossoni M.B., Bastos Neto A.C., Saldanha D.L., Souza V.S., Giovannini A.L., Porto C.G. 2016. Aplicação de técnicas de sensoriamento remoto na investigação do controle do posicionamento do complexo carbonatítico Seis Lagos e no estudo do depósito (Nb) laterítico associado (Amazonas, Brasil). *Pesquisas em Geociências*, **43**(2):111-125. https://doi.org/10.22456/1807-9806.78196

Rossoni M.B., Bastos Neto A.C., Souza V.S., Marques J.C., Dantas E., Botelho N.F., Giovannini A.L., Pereira V.P. 2017. U-Pb zircon geochronologycal investigation on the Morro dos Seis Lagos Carbonatite Complex and associated Nb deposit (Amazonas, Brazil). *Journal of South American Earth Sciences*, **80**:1-17. https://doi.org/10.1016/j.jsames.2017.09.021

Santos J.O.S., Hartmann L.A., Gaudette H.E., Groves D.I., Mcnaughton N.J., Fletcher I.R. 2000. A new understanding of the provinces of the Amazon craton based on integration of field mapping and U-Pb and Sm-Nd geochronology. *Gondwana Research*, **3**(4):453-488. https://doi.org/10.1016/S1342-937X(05)70755-3

Serviço Geológico do Brasil (CPRM). 2006. *Geologia e recursos minerais do estado do Amazonas*. Manaus: CPRM, 125 p.

Simpson R.G. 2012. *Technical report on Aley carbonatite niobium project:* NI 43-101 report prepared for Taseko Mines Ltd. Vancouver: British Columbia, 66 p.

Sinclair A.J., Bentzen A. 1998. Evaluation of errors in paired analytical data by a linear model. *Exploration and Mining Geology*, **7**:167-173.

Takehara L. 2019. *Projeto Avaliação do Potencial de Terras Raras no Brasil:* área Morro dos Seis Lagos, Noroeste do Amazonas. Brasília: CPRM, 112 p.

Thompson M. 1988. Variation of precision with concentration in an analytical system. *Analyst*, **113**(10):1579-1587. https://doi.org/10.1039/AN9881301579

Thompson M., Howarth R.J. 1978. A new approach to the estimation of analytical precision. *Journal of Geochemical Exploration*, **9**(1):23-30. https://doi.org/10.1016/0375-6742(78)90035-3

Van Straaten P. 2002. *Rocks for crops:* agrominerals of Sub-Saharan Africa. Nairobi: International Centre for Research in Agroforestry, 338 p.

Verplanck P.L. 2017. The role of fluids in the formation of rare Earth element deposits. *Procedia Earth and Planetary Science*, **17**:758-761. https://doi.org/10.1016/j.proeps.2017.01.014

Viegas Filho J. de R., Bonow C.W. 1976. *Projeto Seis Lagos:* relatório final. Manaus, CPRM. Available on: http://rigeo.cprm.gov.br/jspui/handle/doc/7601. Accessed on: Apr 30, 2019.

Williams-Jones A.E., Migdisov A.A., Samson I.M. 2012. Hydrothermal mobilisation of the rare Earth elements: a tale of "Ceria" and "Yttria". *Elements*, **8**(5):355-360. https://doi.org/10.2113/gselements.8.5.355

Williams-Jones A.E., Vasyukova O.V. 2018. The economic geology of scandium, the runt of the rare earth element litter. *Economic Geology*, **113**(4):973-988. https://doi.org/10.5382/econgeo.2018.4579

Witt W.K., Hammond D.P., Hughes M. 2019. Geology of the Ngualla carbonatite complex, Tanzania, and origin of the Weathered Bastnaesite Zone REE ore. *Ore Geology Reviews*, **105**:28-54. https://doi.org/10.1016/j.oregeorev.2018.12.002

Woolley A.R. 2001. *Alkaline rocks and carbonatites of the world - Part 3:* Africa. London: The Geological Society of London, **139**, 372 p.